2020

Developing tools to study the clustering-based activation mechanisms of proline-rich tyrosine kinase 2

Shivani Sharma
Iowa State University

Developing tools to study the clustering-based activation mechanisms of proline-rich tyrosine kinase 2

by

Shivani Sharma

A thesis submitted to the graduate faculty

in partial fulfillment of the requirements for the degree of

MASTER OF SCIENCE

Major: Biochemistry

Program of Study Committee:
Eric Underbakke, Major Professor
Richard Honzatko
Vincenzo Venditti

The student author, whose presentation of the scholarship herein was approved by the program of study committee, is solely responsible for the content of this thesis. The Graduate College will ensure this thesis is globally accessible and will not permit alterations after a degree is conferred.

Iowa State University
Ames, Iowa
2020

DEDICATION

To my very loving parents Renu Sharma and Dhiraj Kumar Sharma, and bhai Sagar Sharma, I owe every bit to you!!

TABLE OF CONTENTS

ACKNOWLEDGEMENTS

This work was supported by Grant 1715411 from the National Science Foundation, Division of Molecular and Cellular Biosciences. Firstly, I would like to dedicate a sincere thank you to my advisor and mentor, Dr. Eric Underbakke for his intellectual and emotional support throughout the process. Always encouraging me even during dark and challenging times and never ceasing to stand for me. Nothing would have been possible without his continued assistance. He was always there when I needed any help or had any questions.

Besides my advisor, I would like to thank my POSC committee including Dr. Amy Andreotti, Dr. Kristen Johansen, Dr. Richard Honzatko, Dr. Vincenzo Venditti for their time and willingness to be on my committee and always welcoming my questions.

I was very fortunate to have an amazing lab senior Dr. Hanna Loving, she helped me with any obstacles I faced carrying out an experiment or if I had any questions about anything. The undergrads in the lab who helped by making infinite buffers, doing transformations and various other housekeeping activities that lay the groundwork for every experiment. Also, my friends including Manvi Kapur, Shatabdi Sen, Yukti Dhingra. They were always present for the emotional support I needed and during times of exhaustion, I cannot thank you guys enough for your help.

Last but not the least, my family without whom I would never have been able to pursue my studies in the states at all. My mom for her constant words or encouragement and reminding me that I can do it and to never lose faith in myself. My dad, who always makes sure that I know I am strong enough to face any challenge that comes my way and how to make the best out of it. My brother, who keeps me in check if I am procrastinating or overconfident,

thank you for keeping me grounded and not letting small achievements get to my head too much to stop working hard enough. My dadi who thinks I am the best and no one better exists! My final thanks to the almighty who is making everything possible and makes a way for me even when I feel lost.

ABSTRACT

Pyk2 is a non-receptor tyrosine kinase localized in the postsynaptic density of neurons. As a paralogue of focal adhesion kinase (FAK), Pyk2 shares the FAK domain organization. Both contain an N-terminal FERM (4.1 protein, ezrin, radixin, moesin) domain, linked to a central kinase domain, and a C-terminal FAT (focal adhesion targeting) domain. Despite the domain similarity between FAK and Pyk2, the mechanisms of activation differ strikingly. FAK is canonically activated by recruitment to membrane focal adhesions and phosphoinositide interactions, whereas Pyk2 has adopted sensitivity to Ca^{2+} flux. Understanding the activation mechanism differences will illuminate how gene duplication can generate new signaling responses. The activation of both FAK and Pyk2 involve clustering to promote autophosphorylation in trans. Pyk2 clustering has been reported to be caused by the postsynaptic density scaffolding protein PSD-95. While the regulation and higher-order architecture of the Pyk2—PSD-95 interaction remains unclear, the C-terminal proline-rich repeats of the Pyk2 kinase—FAT linker are implicated in the clustering. Indeed, this region may also be involved in stabilizing a FERM-mediated dimerization interface observed in FAK. The *in vitro* investigation of the scaffolding complex has been limited by protein insolubility, largely due to the large size and putative disorder of the kinase—FAT linker. To enable *in vitro* investigations into the higher-order architecture of the scaffolded Pyk2 activation complex, new Pyk2 expression constructs were developed to promote solubility while encompassing the C-terminal linker and FAT domain. Likewise, constructs for site-specific biotinylation were developed to facilitate binding studies. Together, the new constructs yield soluble proteins for controlled studies of scaffolding architecture and Pyk2 activation.

CHAPTER 1. INTRODUCTION

FAK family non-receptor tyrosine kinases

Pyk2 (proline-rich tyrosine kinase 2) and FAK (focal adhesion kinase) are the only two members of a small family of non-receptor protein tyrosine kinases. Pyk2 appears to have arisen via gene duplication of FAK in chordates (Corsi et al., 2006). Pyk2 – also known as cell adhesion kinase β (CAKβ) (Sasaki et al., 1995), related adhesion focal tyrosine kinase (RAFTK) (Avraham et al., 1995), focal adhesion kinase 2 (FAK2) (Herzog et al., 1996), or calcium dependent protein tyrosine kinase (CADTK) (Yu et al., 1996) – is expressed most abundantly in the brain and hematopoietic cells. In contrast, FAK is expressed ubiquitously. FAK is found in all metazoans and some unicellular eukaryotes. It is a multi-domain, multifunctional protein that outputs cytoplasmic and nuclear responses on receiving and relaying signals from integrins and growth factor receptors. FAK plays an important role in adhesion and migration of cells, a crucial event for cell survival (Schaller, 2010). Other roles of FAK include embryogenesis and wound healing, stemming from the ability of FAK to bypass apoptosis downstream of cell detachment. This makes it a very important candidate for cancer studies due to its role in apoptosis and metastasis. FAK is also involved in multiple cell signaling pathways including phosphatidylinositol 3-kinase (Goñi et al., 2014), AKT1/MAP kinase pathways (S. Park et al., 2004).

Pyk2 signaling in the PSD

While Pyk2 can compensate for FAK function in knockout systems, Pyk2 has apparently developed unique regulatory roles (Weis et al., 2008). Pyk2 is largely cytosolic, with high expression in the central nervous system, specifically in the cerebral cortex, hippocampus, and dentate gyrus etc. (Lev at al., 1995). Pyk2 is involved in key functions in the central nervous system, including neurite outgrowth and synaptic plasticity (Dikic et al., 2000, Huang et al., 2001, Bartos et al., 2010, Hsin et al., 2010). Indeed, Pyk2 is reported to be a risk factor for both Alzheimer's disease and Huntington's disease (Salazar et al., 2019, Giralt et al., 2017). Pyk2 is enriched at the post-synaptic density (PSD) of dendritic spines, a microenvironment of scaffolded signaling proteins responsible for synaptic plasticity signaling.

The activation of Pyk2 is not fully understood, but PSD Ca^{2+}-flux is implicated in activation (Kohno T, Matsuda E, Sasaki A, & Sasaki, 2008). Pyk2 signaling links NMDAR-mediated Ca^{2+} flux to Src signaling cascades that are involved in both synaptic strengthening and weakening (Huang et al., 2001, Hsin et al., 2010). Indeed, catalytically inactive Pyk2 mutants abolish NMDAR currents in rat hippocampal neuronal slices, pointing to a key role in potentiating synaptic NMDARs (Huang et al., 2001).

The Domain Organization of Pyk2 and FAK

Given the shared ancestry, Pyk2 and FAK share a very similar domain organization. Both FAK and Pyk2 are over one thousand residues long. Both contain a central catalytic kinase domain

bounded by an N-terminal FERM domain and a C-terminal FAT domain (Figure 1A). Although structures are reported for various domain truncations of both FAK and Pyk2, the higher-order architecture of these large, multidomain kinases remains unclear (Figure 1B) (Loving & Underbakke, 2019, Han et. al, 2009, Lulo et al., 2009, Lietha et al., 2007).

The FERM domain is named for sequence similarity recognized in forebear domains of protein 4.1, ezrin, radixin, and moesin (Girault et al., 1999). FERM domain can be found in multiple signaling proteins, mediating and regulating intermolecular and intramolecular interactions between proteins and phospholipids. The FERM domain is composed of three subdomains termed the F1, F2 and F3 lobes (Figure 1C). The F1 lobe resembles a ubiquitin-type fold, F2 adopts the acyl-CoA binding protein fold, and the F3 is a PH domain fold (Ceccarelli et al., 2006). The FERM domains of FAK and Pyk2 both regulate the catalytic activity of the kinase through direct interactions between the F2 lobe of the FERM and C-lobe of the kinase (Lietha et al., 2007, Loving & Underbakke 2019). The FERM—kinase interface obscures access to the kinase active site and prevents autophosphorylation of the target FERM—kinase linker tyrosine. Some FERM domains mediate membrane docking with phosphoinositide headgroups via a patch of basic residues between the F1 and F3 subdomains (Hamada et al., 2000). The FAK FERM is also capable of phosphoinositide binding, but an F2 lobe basic patch is implicated in the interaction (Cai et al., 2008, Goni et al., 2014). Interestingly, the phosphoinositide-binding pocket of the radixin FERM appears to be non-functional in FAK, as the basic sidechains are replaced with acidic (Ceccarelli et al., 2006).

FAK and Pyk2 share a classic bilobed kinase catalytic domain with an ATP substrate binding pocket sandwiched between N-terminal and C-terminal lobes (Figure 1C). Regulation of

the kinase involves autoinhibitory interdomain interactions between FERM and kinase domains that block the active site (Lietha et al., 2007, Loving & Underbakke 2019). This interaction apparently sequesters the C-lobe activation loop. Like many protein kinases, activation loop phosphorylation (Y576,Y577 in FAK; Y579,Y580 in Pyk2) promotes the highest levels of phosphotransfer activity (Endicott et al., 2012, Taylor et al., 2011). However, the unphosphorylated activation loop preserves a lower basal activity competent for clustering-induced autophosphorylation during the multi-stage activation mechanisms of FAK and Pyk2 (see below) (Calalb et al., 1995).

The C-terminal FAT domain is a small four-helix bundle that binds to the LD motifs of the focal adhesion scaffold paxillin, among other targets (Walkiewicz et al., 2015). The FAT domain promotes FAK localization to the clustered integrins of a membrane focal adhesion. The Pyk2 FAT domain can also be recruited to focal adhesions, but it is primarily cytosolic (Schaller and Sasaki, 1997). The localization differences may be due to conformational differences or the observation that the Pyk2 FAT–paxillin interaction dissociates more readily (Vanarotti et al., 2014). Intriguingly, the FAK FAT domain was recently implicated in direct regulation of the active conformation of the kinase. FERM-mediated dimers of FAK were stabilized by intermolecular interactions between the FERM F2 basic patch of one monomer and the FAT domain of the other (Brami-Cherrier K et al., 2014). The FAT domain is connected to the kinase via an approximately 180 residue-long, putatively disordered linker. The linker may play scaffolding roles, as it is dotted with several proline-rich regions (PRR, Figure 1A). Indeed, the PRR of Pyk2 are implicated in the clustering-based activation mechanism (see below), although the details remain unclear (Seabold & Hell 2003, Bartos & Hell 2010).

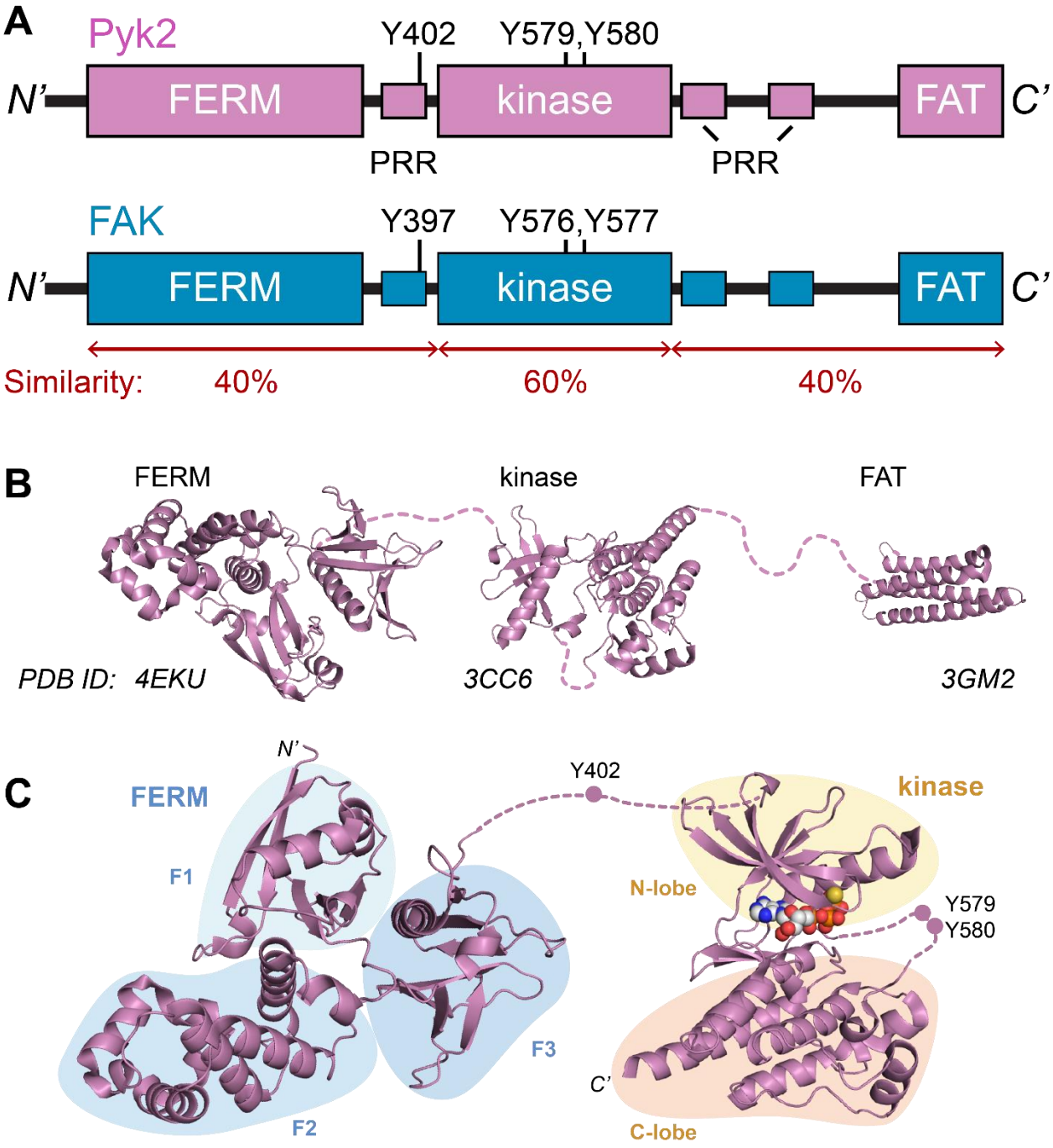

Figure 1.: Domain architecture and sequence similarity of Pyk2 and FAK. **A.** Similarity between Pyk2 (UniprotKB entry Q14289) and FAK (UniprotKB entry Q05397). Tyrosine phosphorylation sites and proline rich regions (PRR) are annotated (adapted from Loving & Underbakke, 2019).**B.** While no structural models are available encompassing the full-length Pyk2, structures of the truncated domains are available, including the FERM (PDB 4eku), kinase (PDB 3cc6, 3fzp, 3fzo), and FAT (PDB 3gm2) (Han et al., 2009, Lulo et al., 2009). **C.** The FERM (PDB

4eku) and ATPγS-bound kinase (PDB 3fzp) are depicted to highlight subdomains and tyrosine phosphorylation sites.

Activation Mechanisms of FAK

The multistep activation mechanism of FAK is relatively well-studied due to its importance in cancer metastasis (Naser et al., 2018, Walkiewicz et al., 2015). While many mechanistic questions remain, FAK and Pyk2 share many features, including a dual role as both signaling enzyme and scaffolding hub. Nevertheless, striking differences in activation control have emerged since the original gene duplication event. Generally, FAK activation involves clustering at the membrane triggered by phosphoinositide lipid interactions. Pyk2 activation is Ca^{2+}-sensitive, and clustering appears to involve a soluble scaffold in neuronal systems (Lev et al., 1995, Bartos & Hell 2010).

FAK activation occurs in multiple, regulated stages. At the lowest, basal activity level FERM—kinase interactions suppress kinase activity (Ceccarelli et al., 2006, Lietha et al., 2007). The autoinhibitory conformation blocks the substrate binding pocket and sequesters the initial site of autophosphorylation. Recruitment to the clustered integrins at membrane focal adhesions via paxillin and talin interactions promotes conformational changes relieving autoinhibition (Cai et al., 2008). This conformational change likely involves FERM-domain interactions with phosphatidylinositol-4,5-bisphosphate generated locally by focal adhesion enzymes (Goni et al., 2014). In addition, mechanical shear forces may contribute to activation, as FAK bridges the extracellular matrix and intracellular actin cytoskeleton (Bauer et al., 2019). The conformational change opening the autoinhibitory FERM—kinase interface is followed by a clustering-facilitated autophosphorylation in trans. Clustering may be a result of the intrinsic

density of the focal adhesion and/or FERM-mediated FAK dimerization. The primary site of autophosphorylation is Y397 in the long FERM—kinase linker. Phospho-Y397 (and a proximal PRR) serve as a docking site and activation trigger for Src tyrosine kinase. Upon Src recruitment to the FAK activation complex, the activation loops of both Src and FAK are mutually phosphorylated to achieve maximal kinase activity.

Activation Mechanisms of Pyk2

Less is known about the Pyk2 activation mechanism. In some cell types and FAK-deficient systems (i.e., knockouts), Pyk2 preserves a vestigial capacity to mimic the FAK activation mechanism (Weis et al., 2008). However, in neuronal systems Pyk2 responds to Ca^{2+}-flux, the frequency and magnitude of which controls the balance of synaptic plasticity. Pyk2 shares a very similar FERM-mediated autoinhibited conformation observed in FAK (Loving & Underbakke, 2019). The activation of Pyk2 is triggered by Ca^{2+}, yet the details remain controversial. The Ca^{2+} sensor calmodulin has been implicated in mechanism (Kohno et al., 2008). Activation by Ca^{2+}/calmodulin may entail dimerization of Pyk2 via direct interaction (Kohno et al., 2008) or multimerization of Pyk2 in the presence of Ca^{2+}/calmodulin using PSD-95 as a soluble scaffold (Kohno et al., 2008, Seabold et al., 2003, Bartos et al., 2010). PSD-95 is one of the most abundant scaffolding proteins found in the PSD. Ca^{2+}-triggered dimerization or scaffolded multimerization induces autophosphorylation of the FERM—kinase linker residue Y402, the residue corresponding to the initial site of FAK autophosphorylation (Figure 1A). Subsequent steps mirror the FAK activation mechanism. Src is recruited to phospho-Y402, and Pyk2 and Src mutually phosphorylate activation loops for maximal kinase activity.

The Ca^{2+}-triggering and clustering remain the most enigmatic stages of the activation mechanism. It has been reported that Pyk2 has a binding site for Ca^{2+}/calmodulin, an alpha-helix (α2) in the F2 FERM subdomain (Kohno et al., 2008). F2 α2 helix is located near the critical FERM F2 lobe hydrophobic pocket that interacts with kinase in the autoinhibited conformation. However, the proposed Ca^{2+}/calmodulin-mediated dimerization mechanism is complicated by the low solvent accessibility of the putative calmodulin binding site.

The scaffolding mechanism based on PSD-95 is an attractive alternative, but the Ca^{2+}-sensitivity is not yet established. The mechanism of Pyk2 oligomerization via PSD-95 can occur in several ways (Bartos et al., 2010). PSD-95 is a multi-domain scaffold presenting many surfaces for protein docking (Figure 2A). PSD-95 may present multiple Pyk2 docking sites within each scaffold, thereby clustering for trans autophosphorylation. However, PSD-95 itself may oligomerize into a higher-order display of docking sites. Palmitoylation of the cysteine residues found close to the N-terminus of PSD-95 (McGee et al., 1999, Qian et al., 2006) and/or intermolecular SH3—GK domain interactions have been proposed to mediate higher-order PSD-95 scaffolding (McGee et al., 2001, Bartos et al., 2010, Kohno et al., 2008, Naser et al., 2018). There is evidence that binding of Pyk2 to PSD-95 is enhanced in the presence of Ca^{2+}/calmodulin (Bartos et al., 2010). High PSD-95 concentrations cause Pyk2 activation in the absence of Ca^{2+}/calmodulin by the same transphosphorylation mechanism, but this is a weaker activation as compared to that in the presence of Ca^{2+}/calmodulin (Bartos et al., 2010). One or more Pyk2 PRRs in the C-terminal kinase—FAT linker interacts with the SH3 domain of PSD-95 (Seabold, et al. 2003, McGee et al. 2001, Tavares et al., 2001). However, this candidate scaffolding interaction is obscured by the GK domain in the native scaffold (Figure 2B).

Nevertheless, PSD-95 induced Pyk2 clustering and activation was reported in neuronal cells (Bartos et al., 2010), and this investigation invoked previous proposals that Ca^{2+}/calmodulin binding to PSD-95 can induce conformational switching to reveal docking sites (Masuko et al., 1999, McGee and Bredt, 1999, McGee et al., 2001).

PSD-95 Structure and Function

PSD-95 (also known as SAP90/MRD62) is encoded by the DLG4 (Disks large homolog 4) gene and a member of the MAGUK (membrane associated guanylate kinase) family. The MAGUK family also includes scaffolding proteins SAP97, SAP102 and PSD93 (Cho et al., 1992, Bredt et al., 1996, Muller et al., 1996). These scaffolding proteins have N-terminal PDZ (PSD-95/Dlg1/ZO-1) domains followed by an SH3 domain, and a GK (guanylate kinase) domain at the C terminus (Figure 2A). The guanylate kinase is catalytically nonfunctional. Dozens of interaction partners have been identified that bind to different domains of PSD-95. The PDZ domains in PSD-95 interact both inter- and intramolecularly with other PDZ domains as well as the C-terminal motifs at the cytosolic termini of transmembrane receptors. These findings were further reviewed by Kim & Sheng (Kim & Sheng, 2004, Kim & Sheng, 2011). The first three PDZ domains of PSD-95 scaffold myriad PSD signaling proteins, such as neurotransmitter receptor subunits, voltage-gated ion channels, neuronal nitric oxide synthase, SynGAP, stargazin family proteins, and Src family kinases. The SH3 domain interacts with Pyk2, an interaction that may compete with intramolecular contacts with the GK domain (Seabold et al., 2003, McGee et al., 2001). The GK domain serves as a docking site for GKAP scaffolds, organizing a higher-order scaffolding

system. PSD-95 is generally a cytosolic scaffold, but palmitoylation cycling is important for regulated recruitment to the PSD (Husseini et al., 2002, Zhang et al., 2014).

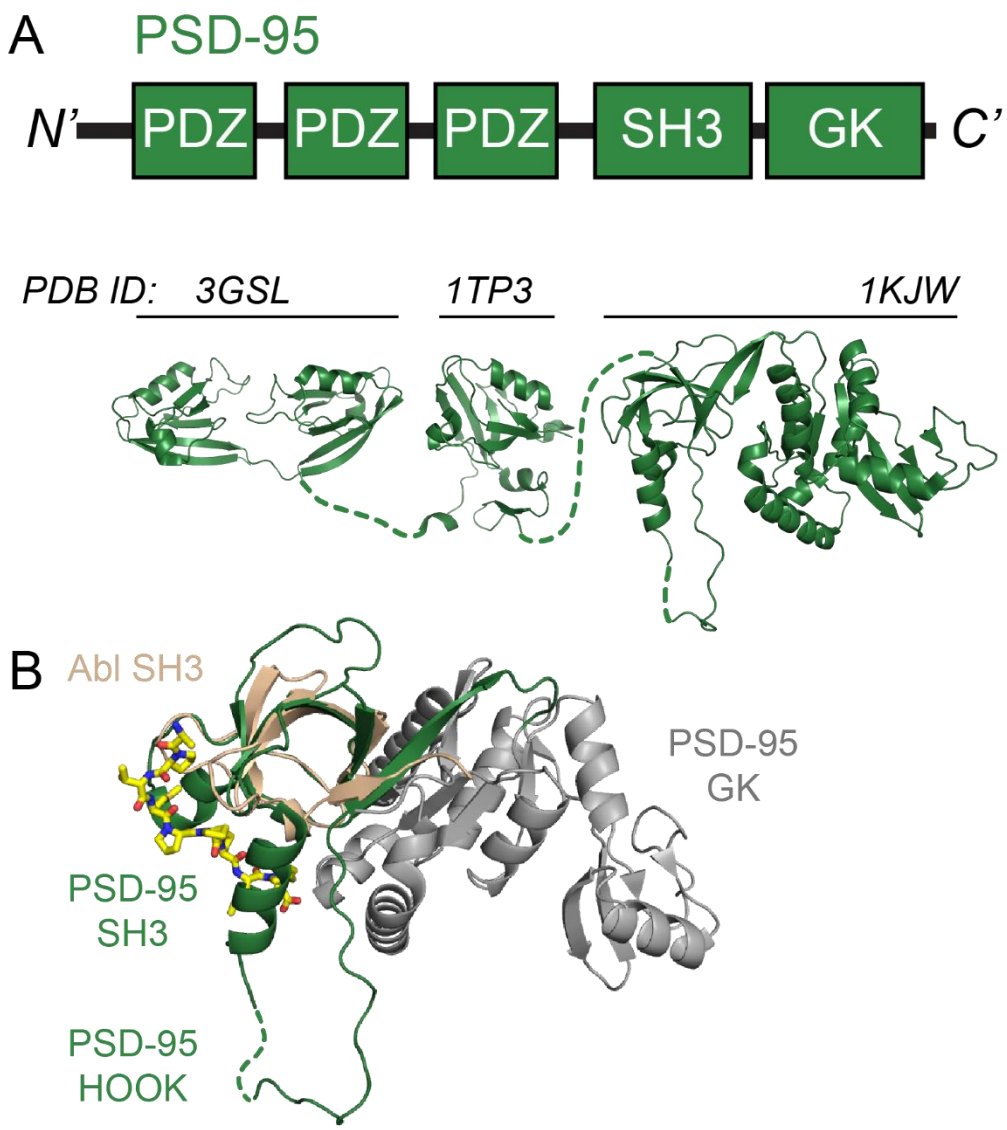

Figure 2. Domain organization of prominent MAGUK scaffold protein PSDPSD-95. **A.** PSDPSD-95 is composed of three N-terminal PDZ domains followed by an SH3 domain and a C-terminal GK domain. A hook-like structure is formed due to intramolecular interaction between and SH3 and GK domain. While no reported structure encompasses the full-length PSD-95, structures are reported for various domain truncations, including PDZ1,2 (PDB 3gsl), PDZ3 (PDB 1tp3), and the SH3-HOOK-GK (PDB 1kjw, 1jxo)(Sainlos et al., 2010, McGee et al., 2001, Tavares et al., 2001). **B.** The HOOK region linking the PSD-95 SH3 (green) and GK (grey) domains may obscure the SH3 binding site for proline-rich peptides (McGee et al., 2001). The canonical SH3 ligand binding site is depicted by alignment of the SH3 domain of Abl kinase bound to a synthetic proline-rich peptide (light brown, PDB 1abo) to the SH3 domain of PSD-95 (PDB 1kjw) (Musacchio et al., 1994).

Goals of our research

The goal of this thesis project is to develop a system to enable the study of the higher-order interactions between Pyk2 and PSD-95. To date, full length Pyk2 has never been purified using recombinant *Escherichia coli* expression systems at the scale necessary for structure-function studies. Efficient recombinant expression and purification of Pyk2 constructs encompassing the three major domains (i.e., FERM, kinase, and FAT) are thwarted by insolubility and aggregation. To enable structural investigations into the Pyk2—PSD-95 clustering complex, we developed two versions of a nearly-full length Pyk2 construct, differing in the number of PRRs but maintaining the overall C-terminal FAT domain. These constructs will drive future work toward a systematic investigation of the role of the Pyk2 C-terminal PRR and FAT domains in scaffolding interactions and FERM-mediated dimerization.

Toward a robust method for investigating scaffolding interactions, we have also developed a system for site-specific biotinylation of PSD-95. Avi tags are minimal recognition motifs for the *E. coli* BirA biotin ligase. We engineered and purified two constructs of PSD-95 with Avi tags introduced at either the N- or C-terminus. Mass spectrometry confirmed efficient and complete biotin conjugation.

References

Avraham, S., London, R., Fu, Y., Ota, S., Hiregowdara, D., Li, J., ... & Avraham, H. (1995). Identification and characterization of a novel related adhesion focal tyrosine kinase (RAFTK) from megakaryocytes and brain. *Journal of Biological Chemistry*, *270*(46), 27742-27751.

Bartos, J., Ulrich, J., Li, H., Beazely, M., Chen, Y., MacDonald, J., & Hell, J. (2010, 1 13). Postsynaptic clustering and activation of Pyk2 by PSD-95. *Journal of Neuroscience, 30*(2), 449-463.

Baucum, A. (2017, 4 19). Proteomic Analysis of Postsynaptic Protein Complexes Underlying Neuronal Plasticity. *ACS Chemical Neuroscience, 8(4)*, 689-701. American Chemical Society.

Bauer, M., Baumann, F., Daday, C., Redondo, P., Durner, E., Jobst, M., . . . Lietha, D. (2019, 4 2). Structural and mechanistic insights into mechanoactivation of focal adhesion kinase. *Proceedings of the National Academy of Sciences of the United States of America, 116*(14), 6766-6774.

Brami-Cherrier, K., Gervasi, N., Arsenieva, D., Walkiewicz, K., Boutterin, M., Ortega, A., . . . Arold, S. (2014, 2 18). FAK dimerization controls its kinase-dependent functions at focal adhesions. *EMBO Journal, 33*(4), 356-370.

Brenman, J., Christopherson, K., Craven, S., McGee, A., Bredt, D., & Klingenstein, J. (1996). *Cloning and Characterization of Postsynaptic Density 93, a Nitric Oxide Synthase Interacting Protein.*

Cai, X., Lietha, D., Ceccarelli, D., Karginov, A., Rajfur, Z., Jacobson, K., . . . Schaller, M. (2008, 1 1). Spatial and Temporal Regulation of Focal Adhesion Kinase Activity in Living Cells. *Molecular and Cellular Biology, 28*(1), 201-214.

Calalb, M., Polte, T., & Hanks, S. (1995). *Tyrosine Phosphorylation of Focal Adhesion Kinase at Sites in the Catalytic Domain Regulates Kinase Activity: a Role for Src Family Kinases.*

Ceccarelli, D., Hyun, K., Poy, F., Schaller, M., & Eck, M. (2006, 1 6). Crystal structure of the FERM domain of focal adhesion kinase. *Journal of Biological Chemistry, 281*(1), 252-259.

Chen, X., Levy, J., Hou, A., Winters, C., Azzam, R., Sousa, A., . . . Reese, T. (2015, 12 15). PSD-95 family MAGUKs are essential for anchoring AMPA and NMDA receptor complexes at the postsynaptic density. *Proceedings of the National Academy of Sciences of the United States of America, 112*(50), E6983-E6992.

Cho, K. O., Hunt, C. A., & Kennedy, M. (1992). The rat brain postsynaptic density fraction contains a homolog of the drosophila discs-large tumor suppressor protein. *Neuron, 9*(5), 929–942.

Corsi, J. M., Rouer, E., Girault, J. A., & Enslen, H. (2006). Organization and post-transcriptional processing of focal adhesion kinase gene. BMC genomics, 7(1), 198.

Dikic, I., Dikic, I., & Schlessinger, J. (1998). *Identification of a New Pyk2 Isoform Implicated in Chemokine and Antigen Receptor Signaling*.*

Ivankovic-Dikic, I., Grönroos, E., Blaukat, A., Barth, B. U., & Dikic, I. (2000). Pyk2 and FAK regulate neurite outgrowth induced by growth factors and integrins. Nature cell biology, 2(9), 574-581.

Dunty, J., & Schaller, M. (2002, 11 22). The N termini of focal adhesion kinase family members regulate substrate phosphorylation, localization, and cell morphology. *Journal of Biological Chemistry, 277*(47), 45644-45654.

Endicott, J., Noble, M., & Johnson, L. (2012, 7 7). The Structural Basis for Control of Eukaryotic Protein Kinases. *Annual Review of Biochemistry, 81*(1), 587-613.

Fan, H., & Guan, J. (2011, 5 27). Compensatory function of Pyk2 protein in the promotion of Focal Adhesion Kinase (FAK)-null mammary cancer stem cell tumorigenicity and metastatic activity. *Journal of Biological Chemistry, 286*(21), 18573-18582.

Goñi, G., Epifano, C., Boskovic, J., Camacho-Artacho, M., Zhou, J., Bronowska, A., . . . Lietha, D. (2014, 8 5). Phosphatidylinositol 4,5-bisphosphate triggers activation of focal adhesion kinase by inducing clustering and conformational changes. *Proceedings of the National Academy of Sciences of the United States of America, 111*(31).

Han, S., Mistry, A., Chang, J., Cunningham, D., Griffor, M., Bonnette, P., . . . Buckbinder, L. (2009, 5 8). Structural characterization of proline-rich tyrosine kinase 2 (PYK2) reveals a unique (DFG-out) conformation and enables inhibitor design. *Journal of Biological Chemistry, 284*(19), 13193-13201.

Hamada, K., Shimizu, T., Matsui, T., Tsukita, S., Tsukita, S., & Hakoshima, T. (2000). Structural basis of the membrane-targeting and unmasking mechanisms of the radixin FERM domain. The EMBO journal, 19(17), 4449-4462.

Herzog, H., Hort, Y. J., & Shine, J. (1996). Molecular cloning and assignment of FAK2, a novel human focal adhesion kinase, to 8p11. 2-p22 by nonisotopic in situ hybridization. Genomics, 32(3).

Hsin, H., Kim, M., Wang, C., & Sheng, M. (2010, 9 8). Proline-rich tyrosine kinase 2 regulates hippocampal long-term depression. *Journal of Neuroscience, 30*(36), 11983-11993.

Huang, Y. Q., Lu, W. Y., Ali, D. W., Pelkey, K. A., Pitcher, G. M., Lu, Y. M., ... & MacDonald, J. F. (2001). CAKβ/Pyk2 kinase is a signaling link for induction of long-term potentiation in CA1 hippocampus. Neuron, 29(2), 485-496.

Husi, H., Ward, M., Choudhary, J., Blackstock, W., & Grant, S. (2000). *Proteomic analysis of NMDA receptor-adhesion protein signaling complexes.*

Kohno, T., Matsuda, E., Sasaki, H., & Sasaki, T. (2008, 3 15). Protein-tyrosine kinase CAKβ/PYK2 is activated by binding Ca 2+/calmodulin to FERM F2 α2 helix and thus forming its dimer. *Biochemical Journal, 410*(3), 513-523.

Lev, S., Moreno, H., Martinez, R., Canoll, P., Peles, E., Musacchio, J. M., ... & Schlessinger, J. (1995). Protein tyrosine kinase PYK2 involved in Ca 2+-induced regulation of ion channel and MAP kinase functions. Nature, 376(6543), 737-745.

Lietha, D., Cai, X., Ceccarelli, D., Li, Y., Schaller, M., & Eck, M. (2007, 6 15). Structural Basis for the Autoinhibition of Focal Adhesion Kinase. *Cell, 129*(6), 1177-1187.

Lim, I., Hall, D., & Hell, J. (2002, 6 14). Selectivity and promiscuity of the first and second PDZ domains of PSD-95 and synapse-associated protein 102. *Journal of Biological Chemistry, 277*(24), 21697-21711.

Loving, H., & Underbakke, E. (2019, 9 10). Conformational Dynamics of FERM-Mediated Autoinhibition in Pyk2 Tyrosine Kinase. *Biochemistry, 58*(36), 3767-3776.

Lulo, J., Yuzawa, S., & Schlessinger, J. (2009). Crystal structures of free and ligand-bound focal adhesion targeting domain of Pyk2. Biochemical and biophysical research communications, 383(3), 347-352.

Martin, S., Grimwood, P., & Morris, R. (2000). *An Evaluation of the Hypothesis.*

Masuko, N., Makino, K., Kuwahara, H., Fukunaga, K., Sudo, T., Araki, N., . . . Saya, H. (1999). *Interaction of NE-dlg/SAP102, a Neuronal and Endocrine Tissue-specific Membrane-associated Guanylate Kinase Protein, with Calmodulin and PSD-95/SAP90 A POSSIBLE REGULATORY ROLE IN MOLECULAR CLUSTERING AT SYNAPTIC SITES* Downloaded from.*

Mcgee, A., & Bredt, D. (1999). *Identification of an Intramolecular Interaction between the SH3 and Guanylate Kinase Domains of PSD-95* Downloaded from.*

McGee, A. W., Dakoji, S. R., Olsen, O., Bredt, D. S., Lim, W. A., & Prehoda, K. E. (2001). Structure of the SH3-guanylate kinase module from PSD-95 suggests a mechanism for regulated assembly of MAGUK scaffolding proteins. Molecular cell, 8(6), 1291-1301.

Mü, B., Kistner, U., & Kindler, S. (1996). *SAP102, a Novel Postsynaptic Protein That Interacts with NMDA Receptor Complexes In Vivo.*

Musacchio, A., Saraste, M., & Wilmanns, M. (1994). *High-resolution crystal structures of tyrosine kinase SH3 domains complexed with praline-rich peptides.*

Naser, R., Aldehaiman, A., Díaz-Galicia, E., & Arold, S. (2018, 6 11). Endogenous control mechanisms of FAK and PYK2 and their relevance to cancer development. *Cancers, 10(6)*. MDPI AG.

Nicodemo, A., Pampillo, M., Ferreira, L., Dale, L., Cregan, T., Ribeiro, F., & Ferguson, S. (2010). Pyk2 uncouples metabotropic glutamate receptor G protein signaling but facilitates ERK1/2 activation. *Molecular Brain, 3*(1).

Qian, Y., & Prehoda, K. (2006, 11 24). Interdomain interactions in the tumor suppressor discs large regulate binding to the synaptic protein GukHolder. *Journal of Biological Chemistry, 281*(47), 35757-35763.

Rao, A., Kim, E., Sheng, M., & Craig, A. (1998). *Heterogeneity in the Molecular Composition of Excitatory Postsynaptic Sites during Development of Hippocampal Neurons in Culture.*

Rao, R., & Finkbeiner, S. (2007). NMDA and AMPA Receptors: Old Channels, New Tricks. *Trends in Neurosciences, 30*(6), 284-291.

Sainlos, M., Tigaret, C., Poujol, C., Olivier, N., Bard, L., Breillat, C., . . . Imperiali, B. (2011). Biomimetic divalent ligands for the acute disruption of synaptic AMPAR stabilization. *Nature Chemical Biology, 7*(2), 81-91.

Sasaki, H., Nagura, K., Ishino, M., Tobioka, H., Kotani, K., & Sasaki, T. (1995). Cloning and characterization of cell adhesion kinase β, a novel protein-tyrosine kinase of the focal adhesion kinase subfamily. *Journal of Biological Chemistry*, *270*(36), 21206-21219.

Schaller, M., & Sasaki, T. (1997). *Differential Signaling by the Focal Adhesion Kinase and Cell Adhesion Kinase *.*

Schaller, M. D. (2010). Cellular functions of FAK kinases: insight into molecular mechanisms and novel functions. *Journal of cell science*, *123*(7), 1007-1013.

Schindler, E., Baumgartner, M., Gribben, E., Li, L., & Efimova, T. (2007, 5). The role of proline-rich protein tyrosine kinase 2 in differentiation- dependent signaling in human epidermal keratinocytes. *Journal of Investigative Dermatology, 127*(5), 1094-1106.

Schlaepfer, D., Hauck, C., & Sieg, D. (1999). *Signaling through focal adhesion kinase PERGAMON.* KOPS.

Seabold, G., Burette, A., Lim, I., Weinberg, R., & Hell, J. (2003, 4 25). Interaction of the tyrosine kinase Pyk2 with the N-methyl-D-aspartate receptor complex via the Src homology 3 domains of PSD-95 and SAP102. *Journal of Biological Chemistry, 278*(17), 15040-15048.

Shin, H., Hsueh, Y.-P., Yang, F.-C., Kim, E., & Sheng, M. (2000). *An Intramolecular Interaction between Src Homology 3 Domain and Guanylate Kinase-Like Domain Required for Channel Clustering by Postsynaptic Density-95/SAP90.*

Taylor, S., & Kornev, A. (2011, 2). Protein kinases: Evolution of dynamic regulatory proteins. *Trends in Biochemical Sciences, 36(2)*, 65-77.

Vanarotti, M., Miller, D., Guibao, C., Nourse, A., & Zheng, J. (2014). Structural and mechanistic insights into the interaction between Pyk2 and paxillin LD motifs. *Journal of Molecular Biology, 426*(24), 3985-4001.

Walkiewicz, K., Girault, J., & Arold, S. (2015, 10 1). How to awaken your nanomachines: Site-specific activation of focal adhesion kinases through ligand interactions. *Progress in Biophysics and Molecular Biology, 119(1)*, 60-71. Elsevier Ltd.

Ivankovic-Dikic, I., Grönroos, E., Blaukat, A., Barth, B. U., & Dikic, I. (2000). Pyk2 and FAK regulate neurite outgrowth induced by growth factors and integrins. Nature cell biology, 2(9), 574-581.

Weis, S. M., Lim, S. T., Lutu-Fuga, K. M., Barnes, L. A., Chen, X. L., Göthert, J. R., ... & Cheresh, D. A. (2008). Compensatory role for Pyk2 during angiogenesis in adult mice lacking endothelial cell FAK. The Journal of cell biology, 181(1), 43-50.

Park, S., Avraham, H., & Avraham, S. (2004). RAFTK/Pyk2 activation is mediated by trans-acting autophosphorylation in a Src-independent manner. *Journal of Biological Chemistry*, *279*(32), 33315–33322. https://doi.org/10.1074/jbc.M313527200

El-Husseini, A. E. D., Schnell, E., Dakoji, S., Sweeney, N., Zhou, Q., Prange, O., ... & Bredt, D. S. (2002). Synaptic strength regulated by palmitate cycling on PSD-95. Cell, 108(6), 849-863.

Zhang, Y., Matt, L., Patriarchi, T., Malik, Z. A., Chowdhury, D., Park, D. K., ... & Hell, J. W. (2014). Capping of the N-terminus of PSD-95 by calmodulin triggers its postsynaptic release. The EMBO journal, 33(12), 1341-1353.

Salazar, S. V., Cox, T. O., Lee, S., Brody, A. H., Chyung, A. S., Haas, L. T., & Strittmatter, S. M. (2019). Alzheimer's disease risk factor Pyk2 mediates amyloid-β-induced synaptic dysfunction and loss. Journal of Neuroscience, 39(4), 758-772.

Giralt, A., Brito, V., Chevy, Q., Simonnet, C., Otsu, Y., Cifuentes-Díaz, C., ... & Poncer, J. C. (2017). Pyk2 modulates hippocampal excitatory synapses and contributes to cognitive deficits in a Huntington's disease model. Nature communications, 8(1), 1-16.

Girault, J. A., Labesse, G., Mornon, J. P., & Callebaut, I. (1999). The N-termini of FAK and JAKs contain divergent band 4.1 domains. *Trends in biochemical sciences*, *24*(2), 54-57.

Kim, E., & Sheng, M. (2004). PDZ domain proteins of synapses. *Nature Reviews Neuroscience*, *5*(10), 771-781.

Sheng, M., & Kim, E. (2011). The postsynaptic organization of synapses. *Cold Spring Harbor perspectives in biology*, *3*(12), a005678.

Tavares, G. A., Panepucci, E. H., & Brunger, A. T. (2001). Structural characterization of the intramolecular interaction between the SH3 and guanylate kinase domains of PSD-95. *Molecular cell*, *8*(6), 1313-1325.

Yu, H., Li, X., Marchetto, G. S., Dy, R., Hunter, D., Calvo, B., ... & Earp, H. S. (1996). Activation of a Novel Calcium-dependent Protein-tyrosine Kinase CORRELATION WITH c-Jun N-TERMINAL KINASE BUT NOT MITOGEN-ACTIVATED PROTEIN KINASE ACTIVATION. *Journal of Biological Chemistry*, *271*(47), 29993-29998.

CHAPTER 2: SITE-SPECIFIC BIOTINYLATION OF PSD-95

Shivani Sharma and Eric Underbakke

From the Roy J. Carver Department of Biochemistry, Biophysics and Molecular Biology, Iowa State University, Ames, Iowa 50011

Modified from a manuscript in preparation for bioRxiv

Abstract

Pyk2 activation involves scaffolded clustering for efficient autophosphorylation in trans. The scaffold protein PSD-95 has been implicated in the clustering-based activation of Pyk2 in the post-synaptic density (PSD). Indeed, the SH3 domain of PSD-95 is known to interact with proline-rich repeats (PRRs) of the Pyk2 C-terminus. Nevertheless, questions about the clustering mechanism remain. For instance, does PSD-95 present additional Pyk2 docking sites for dimerization or is a higher-order assembly responsible for clustering? To probe the binding interactions underlying the Pyk2 scaffolded activation complex, we sought a method for robust and stable surface or bead immobilization of PSD-95. Biotin labeling using Avi tags is versatile strategy for binding protein immobilization due to the extremely high affinity ($K_D \sim 10^{-15}$ M) of biotin for the avidin family of biotin-binding proteins. We engineered expression constructs encoding His-SUMO-tagged full-length PSD-95 with the addition of either an N-terminal or C-terminal Avi tag. Avi-tagged PSD-95 was expressed and purified, and the BirA biotin ligase was used for site-specific biotin conjugation. Biotinylation conditions were optimized to drive the reaction to completion, as confirmed by intact protein mass spectrometry. We anticipate that

the biotinylated PSD-95 will be instrumental for future Pyk2 binding studies using surface plasmon resonance and immobilized avidin pull-downs.

Introduction

Pyk2 kinase activity is linked to regulation of synaptic plasticity through Src activation and NMDA receptor phosphorylation (Lu et al., 1998, Yu et al., 1996, Seabold et al., 2003, Hsin et al., 2010, Bartos et al., 2010). Hell and co-workers have established that the PSD scaffold PSD-95 and its homologue SAP102 are responsible for localizing Pyk2 and Src to the NMDA receptors (Seabold et al., 2003). This PSD-95-mediated scaffolding is also critical for clustering Pyk2 for trans autophosphorylation during Ca^{2+} flux (Bartos et al., 2010). Proline-rich repeats (PRR) in the Pyk2 C-terminal linker appear to dock with the SH3 domain of PSD-95 (Seabold et al., 2003). Intruigingly, the presence of the PSD-95 GK domain occludes the SH3—PRR interaction (Seabold et al., 2003, Tavares et al., 2001, McGee et al., 2001). The alternative, mutually exclusive SH3 interactions (i.e., intermolecular SH3—Pyk2 PRR vs. intramolecular SH3—GK) were proposed as a possible point of regulation for Ca^{2+} sensitivity (Bartos et al., 2001). For example, Ca^{2+}-calmodulin may bind to the HOOK region between the PSD-95 SH3 and GK domains, rearranging the intramolecular interaction to reveal the SH3 docking site for the Pyk2 PRR (Fukunaga et al., 2005). Nevertheless, a mechanistic basis for Ca^{2+}-dependent Pyk2 scaffolding remains to be determined.

As Pyk2 autophosphorylation in trans is a critical step in the early stages of Pyk2 activation, clustering of Pyk2 by PSD-95 is a compelling mechanism for inducement of autophosphorylation (Bartos et al., 2001). Indeed, the intrinsic kinase activity of the unphosphorylated Pyk2 is relatively low, and increased local concentration due to scaffolded

clustering could initiate productive autophosphorylation (Loving & Underbakke, 2019). To date, the only reported Pyk2 docking site on PSD-95 is the SH3 domain (Seabold et al., 2003). It remains unclear how PSD-95 could scaffold multiple copies of Pyk2 for productive clustering. Two mechanisms for higher-order scaffolding are possible: i. PSD-95 may present a second binding site, or ii. PSD-95 may dimerize/oligomerize to form a higher-order scaffodling structure. In support of higher-order PSD-95 oligomerization, SH3-GK domain swapping has been proposed as a mechanism (Masuko et al., 1999, Nix et al., 2000, McGee et al., 2001). In addition, palmitoylation of cysteine(s) in the N-terminus of PSD-95 has been reported to promote oligomerization (Craven et al., 1999, Husseini et al., 2000, Zhang et al., 2014). However, alternative PSD-95 docking sites are also a possibility, as Pyk2 constructs missing the C-terminal PRR are also activated by PSD-95-mediated clustering (Loving & Underbakke, unpublished data).

Further investigations into the scaffolding of Pyk2 by PSD-95 could resolve the ambiguouities surrounding the Ca^{2+}-induced, clustering-based activation mechanism. We aimed to develop binding affinity assays to study the same interaction. Preliminary qualitative pull-down binding assays using standard protein purification affinity tags (His_6 or GST) suffered from low specificity and irreproducibility (data not shown). Nevertheless, immobilization on beads (pull-downs) or surfaces (surface plasmon resonance (SPR) biosensors) is an attractive option for systematic studies of binding interactions. We chose to employ the widely used interaction between biotin and avidin family proteins (**Figure 3A**). The binding of biotin to avidin or streptavidin is one of the strongest known non-covalent interactions (K_D ~10^{-14} – 10^{-15}) (Weber et al., 1989). The biotin—avidin system has been used extensively in the biotechnology for

binding interaction studies, proximity labeling, cell imaging, and DNA origami. In comparison to other affinity tags, the biotin-avidin immobilization confers multiple advantages for SPR and pull down experiments, including exceptionally low binding off rate, high specificity, and the ability to withstand stringent washes. One disadvantage is that biotin is not directly genetically encoded, necessitating a conjugation step. While side-chain reactive biotin conjugation is widely available, we sought a site-specific strategy for immobilization control. The *E. coli* biotin ligase BirA catalyzes the conjugation of ATP-activated biotin to a Lys residue within a specific recognition motif (e.g.,. GLNDIFEAQKIEWHE) (**Figure 3B**) (Barker & Campbell, 1981, Schatz, 1993, Beckett et al., 1999). This recognition motif has been fused with many proteins in expression vectors for a small, genetically-encoded biotinylation site known as an Avi tag.

We chose to engineer BirA biotinylation motifs (i.e., Avi tags) at either the N- and C-terminii of PSD-95. Having each terminus labeled would enable binding experiments where each end of the scaffold would be maximally free for protein docking. Here, we report the design, purification, and sucessful BirA-mediated biotinylation of Avi-tagged PSD-95.

Materials and Methods

Plasmids

Plasmids templates were obtained from the following sources. Cloning vector pBAD His6 TEV LIC cloning vector (8B) was a gift from Scott Gradia (Addgene plasmid # 37502). The pBAD-H6-SUMO-PSD95 plasmid, a derivative of 8B, was cloned by Dr. Hanna Loving (Underbakke lab). Saccharomyces cerevisiae SUMO protease H6-Ulp1 (residues 423−621) expression vector

pHYRS52 received as a gift from H. Iwai (Addgene, 31122). The pSV272 expression vector for BirA was obtained from the lab of Dipali Sashital.

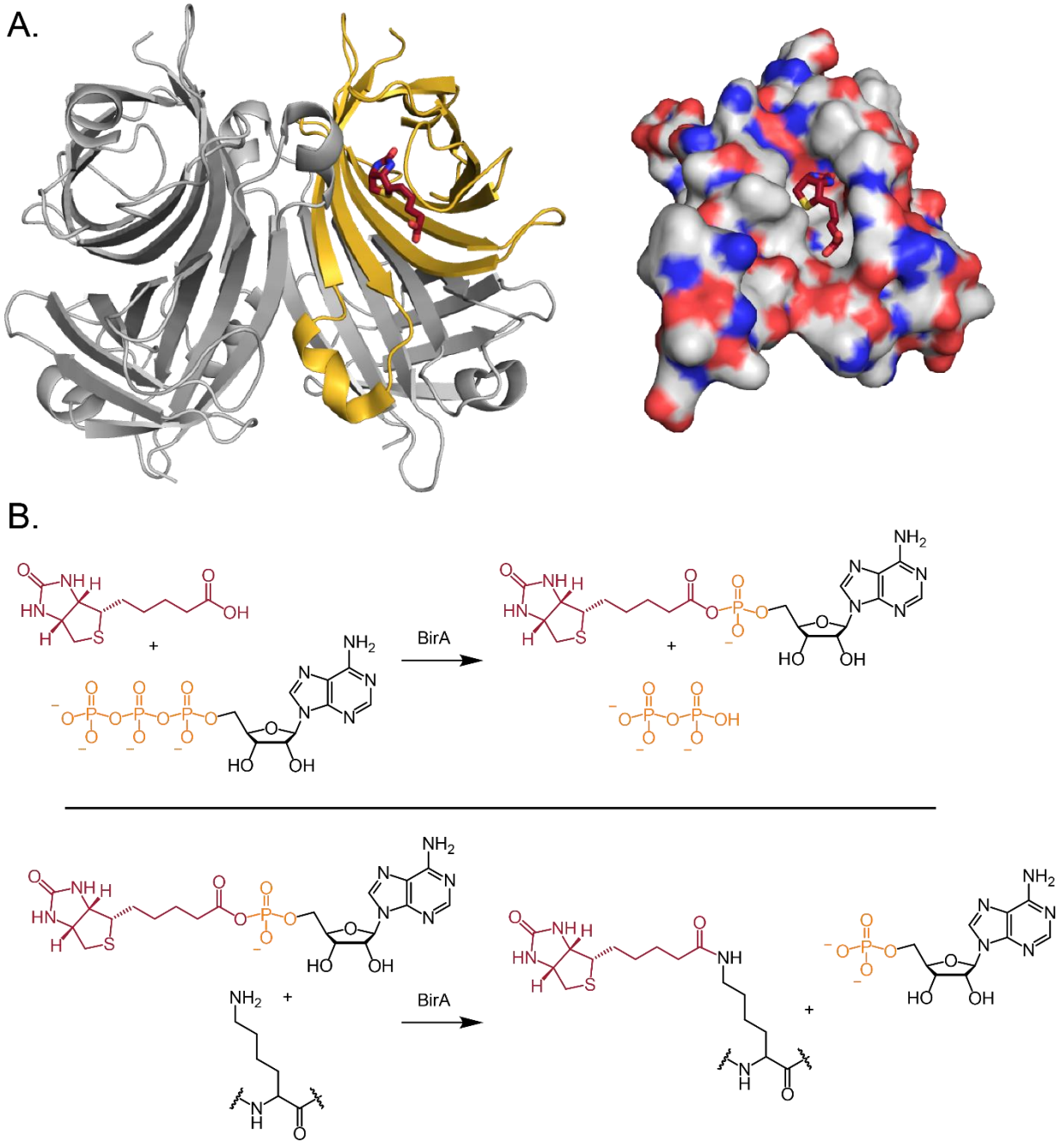

Figure 3. Biotinylation and high affinity binding with streptavidin. **A.** Biotin binds to tetrameric streptavidin (left). Streptavidin monomer is highlighted in gold with bound biotin in cardinal red. The binding affinity is unusally high due to extensive van der Walls interactions, ordering of

protein loops to envelope the biotin, and hydrogen bonds deep in the binding crevice (right). **B.** The *E. coli* biotin ligase BirA conjugates biotin to a Lys within a consensus recognition sequence using an activated biotinyl-AMP intermediate.

Generating Avi-tagged PSD-95 expression vectors pSS001 and pSS002

The 'Round the Horn PCR-based mutagenesis strategy was used to incorporate primer-encoded Avi tags in frame with the N-terminus or C-terminus of PSD-95 in the expression vector pBAD-H6-SUMO-PSD95. Primers used to generate the N-terminal Avi-tagged construct (EU134/EU135, pSS002) and C-terminal Avi-tagged construct (EU132/133, pSS001) are listed in **Table 1**. Primers for PCR-based introduction of C- or N-terminal Avi-tags in frame with PSD-95 in the pBAD-H6-SUMO-PSD95 expression vector to generate pSS001 and pSS002, respectively.

Primer Name	Description	Sequence (3' to 5')
EU132	C-terminal Avi tag forward primer	CTCAGAAAATCGAGTGGCATGAATAACGGATCCCTTG GCTGTTTTGGCGG
EU133	C-terminal Avi tag reverse primer	CCTCAAAAATGTCATTCAGACCGGACAGTCTCTCTC GGGCTGGGACCC
EU134	N-terminal Avi tag forward primer	GGCTCAGAAAATCGAGTGGCATGAAGGTGACACG CCCCCTCTGGAACACAGC
EU135	N-terminal Avi tag reverse primer	TCAAAAATGTCATTCAGACCGGACCCACCAATCTG TTCTCTGTGAGCCTC

The primers were prepared for downstream ligation by 5' phosphorylation using T4 polynucleotide kinase (PNK) incubated with 10 mM ATP at 37 °C for 30 min. PNK was heat inactivated at 65 °C for 20 min. Primer pairs were used to amplify template pBAD-H6-SUMO-PSD95 using standard PCR conditions for Phusion DNA polymerase (New England Biolabs). Expected product sizes (8.1 kbp) were checked by diagnostic DNA agarose gel. Successful PCR reactions were pooled, and template was digested using DpnI restriction enzyme (2 hrs, 37 °C).

Blunt-ended, linear PCR product was circularized using T4 DNA ligase (Thermo Scientific) during an 18 hrs, 25 °C incubation. The ligation reaction was transformed into DH5α chemically competent *E. coli* by heat shock transformation. Transformants were selected by plating on LB supplemented with 100 µg/mL ampicillin. Ampicillin-resistant transformants were grown in small ampicillin-supplemented LB cultures, and plasmids were isolated using Wizard Plus SV Miniprep kits (Promega). Successful introduction of the Avi tags was confirmed using DNA sequencing. The C-terminal Avi tag construct was designated pSS001, the N-terminal pSS002.

Purification of Avi-tagged PSD-95

Expression plasmids pSS001 and pSS002 encoding pBAD-H6-SUMO-PSD95-Avi-tag and pBAD-H6-SUMO-Avi-tag-PSD95, respectively, were transformed into C41(DE3) cells. Starter cultures were grown overnight at 37 °C using LB medium containing 50 µg/mL ampicillin. The starter culture was used to inoculate four 1 L expression cultures (1:100) of LB with 50 µg/mL ampicillin. Expression cultures were grown at 37 °C with continuous shaking until they reach an OD_{600nm} of 0.30, at which time the temperature was decreased to 18 °C. Once cells reach an OD_{600nm} of 0.5, the cells were induced with 0.02% Arabinose (final concentration) and left to shake overnight at 18 °C. Harvesting of cells is completed after 18 hr using centrifugation at 4,200 ×g for 20 min. Cell pellets were stored at −80 °C until used for purification. Harvested cells were thawed after addition of lysis buffer (50 mM Tris pH 8, 20 mM imidazole, 50 mM KCl, 10% glycerol, 1 mM 2-mercaptoethanol, 1 mM phenylmethylsulfonyl fluoride). Cells were lysed using sonication. The lysate is centrifuged at 20,000 ×g for 45 min at 4 °C to remove cell debris. Cleared lysate was passed through a HisPur Ni-NTA Superflow agarose column (2 mL of resin, Thermo Scientific) equilibrated in binding buffer (50 mM Tris pH 8, 20 mM imidazole, 50 mM

KCl, 10% glycerol, 1 mM 2-mercaptoethanol). The Ni-NTA column was washed with 12 column volumes of wash buffer (50 mM Tris pH 8, 20 mM imidazole, 200 mM KCl, 10% glycerol, 1 mM 2-mercaptoethanol pH 8). H6-SUMO-Avi-tagged PSD-95 was eluted with high-imidazole elution buffer (50 mM Tris pH 8, 300 mM imidazole, 100 mM KCl, 10% glycerol, 1 mM 2-mercaptoethanol). Fractions containing our protein were dialyzed for 3 hr with H6-Ulp1 (a SUMO-specific protease) using the dialysis buffer (50 mM Tris pH 7.8, 100 mM KCl, 5% glycerol, 1 mM DTT). A subtractive run through the Ni-NTA column re-equilibrated in binding buffer followed for the removal of purification tags and H6-Ulp1. PSD-95 constructs were further buffer exchanged by passing through a Bio-Scale Mini Bio-Gel P-6 desalting cartridge (Bio-Rad) pre-equilibrated in storage buffer (150 mM NaCl, 50 mM HEPES, 10% glycerol, and 1 mM DTT pH 7.4). Protein was concentrated using a Spin-X concentrator of 10k MWCO (Corning), aliquoted, and snap-frozen in liquid N_2. Protein stocks were stored at −80 °C.

Purification pf BirA

Expression plasmid pSV272:BirA encoding H6-MBP-TEV-BirA, was transformed into C41(DE3) cells. Starter cultures were grown overnight at 37 °C using LB medium containing 50 µg/mL kanamycin. The starter culture was used to inoculate four 1 L expression cultures (1:100) of LB with 50 µg/mL kanamycin. Expression cultures were grown at 37 °C with continuous shaking until they reach an OD_{600nm} of 0.30, at which point the temperature was decreased to 18 °C. Once cells reach an OD_{600nm} of 0.5, the cells were induced with 1 mM isopropyl β-D-1-thiogalactopyranoside and left to shake overnight at 18 °C. Harvesting of cells was completed using centrifugation at 4,200 ×g for 20 min. Cell pellets were stored at −80 °C until purification. Frozen cells were thawed after addition of lysis buffer (25 mM Tris, 200 mM NaCl, pH 8.0 and 5

mM 2-mercaptoethanol). Cells were lysed using sonication. The lysate is centrifuged at 20,000 ×g for 45 min at 4 °C to remove cell debris. Cleared lysate was passed through a HisPur Ni-NTA Superflow agarose column (2 mL of resin, Thermo Scientific) equilibrated in binding buffer (25 mM Tris pH 8, 200 mM NaCl, 20mM imidazole, 5 mM 2-mercaptoethanol). The Ni-NTA column was washed with 12 column volumes of wash buffer (250mM NaCl, 50mM Tris pH 8, 5% glycerol, 20mM imidazole, and 5 mM 2-mercaptoethanol). His-MBP-tagged BirA was eluted with high-imidazole elution buffer (25 mM Tris pH 8.0, 200 mM NaCl, 400 mM imidazole, and 5 mM 2-mercaptoethanol). Fractions containing our protein were dialyzed overnight with GFP-TEV, a protease specific to the TEV motif engineered between His-MBP and BirA sequences in this construct. Dialysis buffer was composed of 50 mM Tris pH 7.8, 100 mM KCl, 5% glycerol, 1 mM DTT. A subtractive run through the Ni-NTA column (re-equilibrated in binding buffer) followed for the removal of purification tags and GFP-TEV. were further buffer exchanged by passing through a Bio-Scale Mini Bio-Gel P-6 desalting cartridge (Bio-Rad) pre-equilibrated in storage buffer (150 mM NaCl, 50 mM HEPES, 10% glycerol, and 1 mM DTT pH 7.4). Protein was concentrated using a Spin-X concentrator of 10k MWCO (Corning), aliquoted, and snap-frozen in liquid N_2. Protein stocks were stored at −80 °C.

Biotinylation of Avi-tagged PSD-95

Biotinylation of purified Avi-tagged PSD-95 was performed by incubating BirA, biotin, and ATP at 30 °C for 30 min with gentle rocking. Reactions were composed of 5 µM Avi-tagged PSD-95, 0.5 µM BirA, 5 mM ATP, 0.15 mM biotin, in a biotinylation buffer composed of 50 mM HEPES pH 7.4, 150 mM NaCl, 5 mM $MgCl_2$, 5 mM DTT (final concentrations). At various time points (15

min, 30 min, 1 hr, 2 hr), biotinylation reactions were quenched by the addition of EDTA to a final concentration of 10 mM. Quenched biotinylated samples were passed through the desalting column to remove excess biotin and ATP.

Mass spectrometry of biotinylated PSD-95

The extent of biotinylation was assessed using intact protein mass spectrometry. The quenched biotinylation reaction was diluted to 1 µM protein and injected (10 µL) into an ACQUITY UPLC H-class coupled in-line to an ESI-Q-TOF Synapt G2-Si (Waters). Mobile phases consisted of solvents A (HPLC-grade aqueous 0.1% formic acid) and B (HPLC-grade acetonitrile, 0.1% formic acid). Exchange samples were resolved on a C4 column (5 µm, 1 × 50 mm; Restek) at 400 µL/min flow rate using the following gradient: 0–1 min 10% B, 1–4 min 10 – 75% B, 4-6 min 75—100% B. MS data was collected in positive ion, MS continuum, resolution mode with an m/z range of 300 – 4,000.

Results and Discussion

Design and engineering of Avi-tagged PSD-95 expression vectors

For the N-terminal fusion, the Avi tag primer was engineered downstream of the His-SUMO tag in order to retain the tag after the affinity/solubility H6-SUMO tag is cleaved by the protease Ulp1. The primers encode the tag (split between forward and reverse primers) and sequence complementary to the template for annealing and extension.

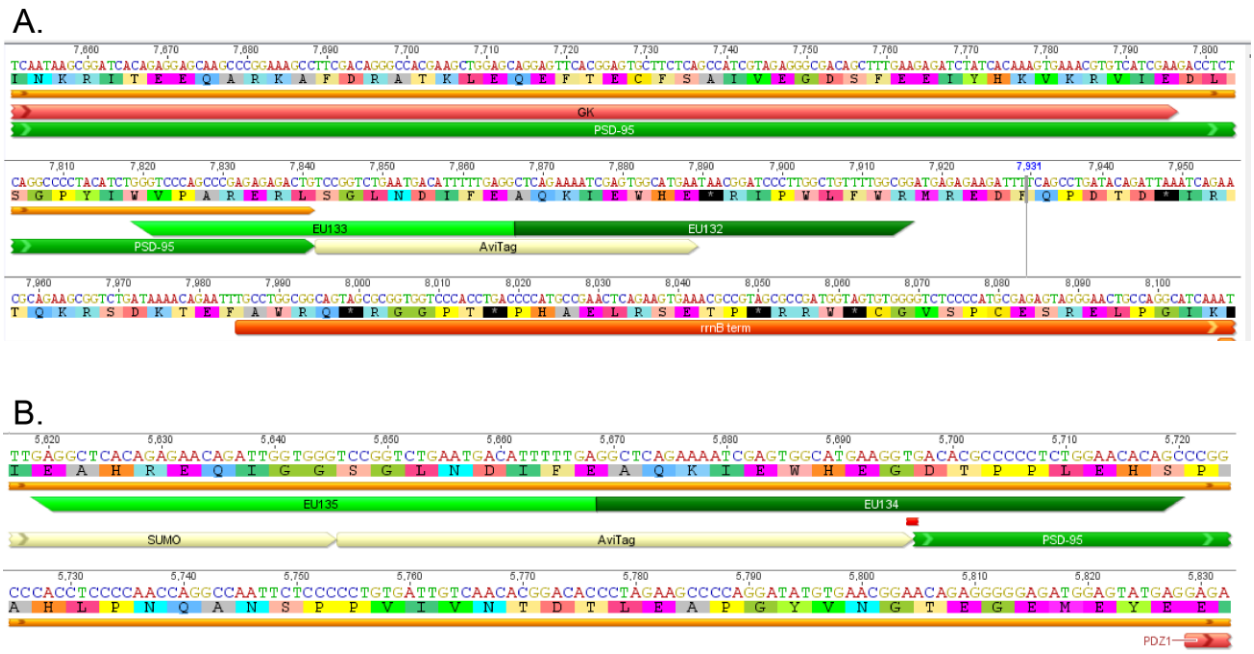

Figure 4. Design of 'Round-the-Horn primers encoding Avi-tags for pSS001 (**A**) and pSS002 (**B**). Aligned primers and domains are annotated below nucleic acid and protein sequences.

Purification of Avi-tagged PSD-95

Avi-tagged PSD was expressed recombinantly in *E. coli* cells using an arabinose expression system from pSS001 or pSS002. Proteins were purified by leveraging the N-terminal His_6-SUMO affinity/solubility tag. Immobilized metal affinity chromatography (IMAC) enriched the tagged PSD-95, and the His_6-SUMO tag was removed with treatment with His_6-Ulp. The free His_6-SUMO tag, His_6-Ulp1, and residual background *E. coli* proteins were further removed with a subtractive IMAC run. Purification yields were typically 100 µM or 2 mg per liter of expression media (**Figure 5A**).

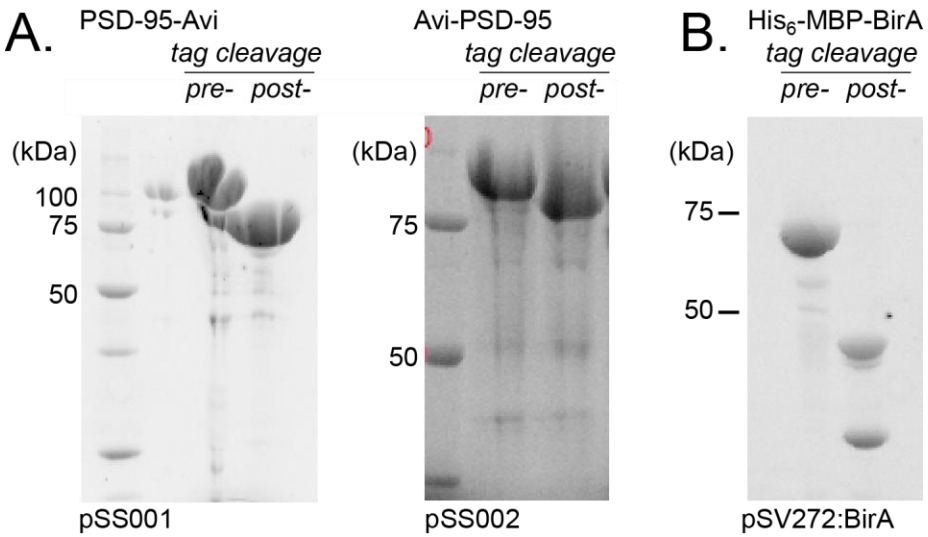

Figure 5. Purification of Avi-tagged PSD-95 and BirA. **A**. PSD-95 with a C-terminal Avi tag (PSD-95-Avi, a product of pSS001) and PSD-95 with an N-terminal Avi tag (Avi-PSD-95 from pSS002) were resolved by SDS-PAGE pre- and post-His_6-SUMO tag cleavage with Ulp1. Expected molecular weights are 95,021 Da and 82,000 Da pre- and post-cleavage, respectively, for PSD-95-Avi. For Avi-PSD-95 expected molecular weights are 92,986 Da and 79,966 Da for pre- and post-tag cleavage, respectively. **B.** Purified BirA was resolved by SDS-PAGE pre- and post-cleavage of the MBP tag by TEV protease. Expected molecular weights are 79,831 Da pre-cleavage, and 35,369 Da post-cleavage. The free MBP tag is 44,480 Da.

To optimize biotinylation conditions, we started by producing the biotin ligase BirA. The His_6-MBP-tagged BirA expression vector (pSV272:BirA) was a gift from the lab of Dipali Sashital. Briefly, His_6-MBP-BirA was enriched by IMAC. The His_6-MBP tag was cleaved by TEV protease, and tags, TEV protease, and non-specific *E. coli* Ni-binding proteins were removed with a subtractive IMAC run (**Figure 5B**). Typical BirA yields were ~280 µM, ~3 mg per liter of expression media.

Biotinylation reactions were optimized by adapting the procedure of Li & Sousa (Li & Sousa, 2012). Briefly, Avi-tagged PSD-95 was incubated for various times with biotin, Mg^{2+}:ATP, and

catalytic quantities of BirA. Reactions were quenched with EDTA and buffer exchanged using a desalting gel filtration column to remove excess biotin and ATP.

The extent of biotinylation was assessed using intact protein liquid chromatography-coupled electrospray mass spectrometry (LC-ESI-MS). Partial biotinylation is evident at 15 min, and biotinylation appears to be complete within 30 min (**Figure 6**). Taken together, the data indicated that the Avi-tagged full-length PSD-95 constructs developed herein are soluble and purify with yields sufficient for extensive structure-function characterization. PSD-95 constructs underwent complete and rapid biotinylation. We anticipate that these proteins will empower quantitative investigations into the interactions with Pyk2 and the assembly of the higher-order activation complex. With biotin-conjugates at both N- and C-termini, SPR experiments will be forthcoming for determining the k_{on} and k_{off} of Pyk2 and various Pyk2 domain truncations. We also expect that these expression constructs will serve as a platform for PSD-95 domain truncations and point mutations for mapping and localizing docking interface hot spots.

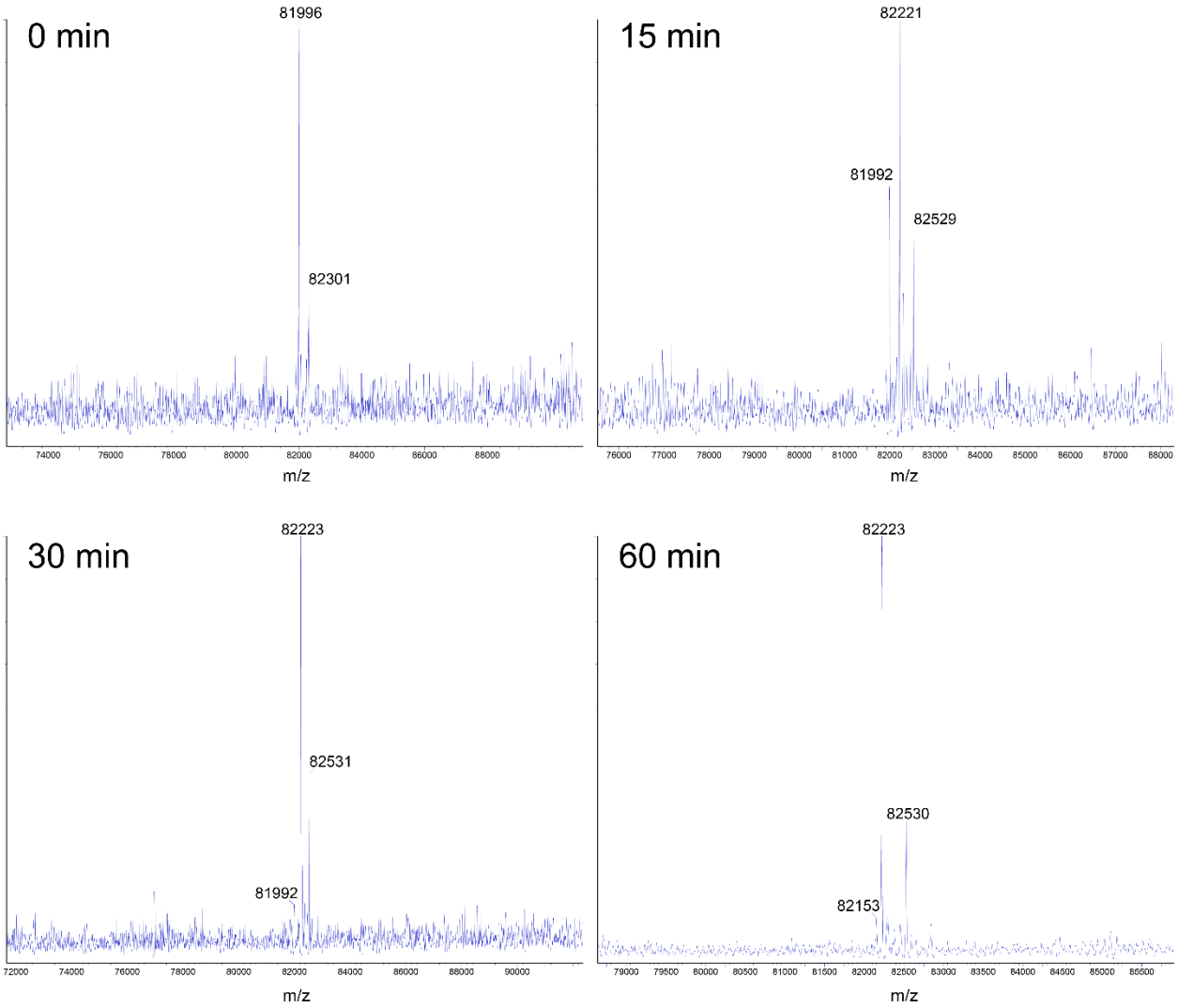

Figure 6. Representative spectra of PSD-95-Avi biotinylation reaction time points. Quenched reaction samples at various time points were analyzed by LC-ESI-MS. Expected molecular weights were 82,000 Da for the apo PSD-95-Avi and 82,226 Da for biotinylated-PSD-95-Avi. Observed m/z exhibited <5 ppm deviation from expected m/z.

References

Seabold, G. K., Burette, A., Lim, I. A., Weinberg, R. J., & Hell, J. W. (2003). Interaction of the tyrosine kinase Pyk2 with the N-methyl-D-aspartate receptor complex via the Src homology 3 domains of PSD-95 and SAP102. Journal of Biological Chemistry, 278(17), 15040-15048.

Bartos, J. A., Ulrich, J. D., Li, H., Beazely, M. A., Chen, Y., MacDonald, J. F., & Hell, J. W. (2010). Postsynaptic clustering and activation of Pyk2 by PSD-95. Journal of Neuroscience, 30(2), 449-463.

Loving, H. S., & Underbakke, E. S. (2019). Conformational dynamics of FERM-mediated autoinhibition in Pyk2 tyrosine kinase. Biochemistry, 58(36), 3767-3776.

Lu, Y. M., Roder, J. C., Davidow, J., & Salter, M. W. (1998). Src activation in the induction of long-term potentiation in CA1 hippocampal neurons. *Science*, *279*(5355), 1363-1368.

Yu, H., Li, X., Marchetto, G. S., Dy, R., Hunter, D., Calvo, B., ... & Earp, H. S. (1996). Activation of a Novel Calcium-dependent Protein-tyrosine Kinase CORRELATION WITH c-Jun N-TERMINAL KINASE BUT NOT MITOGEN-ACTIVATED PROTEIN KINASE ACTIVATION. *Journal of Biological Chemistry*, *271*(47), 29993-29998.

Hsin, H., Kim, M. J., Wang, C. F., & Sheng, M. (2010). Proline-rich tyrosine kinase 2 regulates hippocampal long-term depression. *Journal of Neuroscience*, *30*(36), 11983-11993.

Fukunaga, Y., Matsubara, M., Nagai, R., & Miyazawa, A. (2005). The interaction between PSD-95 and Ca2+/calmodulin is enhanced by PDZ-binding proteins. *Journal of biochemistry*, *138*(2), 177-182.

Masuko, N., Makino, K., Kuwahara, H., Fukunaga, K., Sudo, T., Araki, N., ... & Saya, H. (1999). Interaction of NE-dlg/SAP102, a neuronal and endocrine tissue-specific membrane-associated guanylate kinase protein, with calmodulin and PSD-95/SAP90 a possible regulatory role in molecular clustering at synaptic sites. *Journal of Biological Chemistry*, *274*(9), 5782-5790.

McGee, A. W., Dakoji, S. R., Olsen, O., Bredt, D. S., Lim, W. A., & Prehoda, K. E. (2001). Structure of the SH3-guanylate kinase module from PSD-95 suggests a mechanism for regulated assembly of MAGUK scaffolding proteins. *Molecular cell*, *8*(6), 1291-1301.

Nix, S. L., Chishti, A. H., Anderson, J. M., & Walther, Z. (2000). hCASK and hDlg associate in epithelia, and their src homology 3 and guanylate kinase domains participate in both intramolecular and intermolecular interactions. *Journal of biological chemistry*, *275*(52), 41192-41200.

Tavares, G. A., Panepucci, E. H., & Brunger, A. T. (2001). Structural characterization of the intramolecular interaction between the SH3 and guanylate kinase domains of PSD-95. *Molecular cell*, *8*(6), 1313-1325.

Craven, S. E., El-Husseini, A. E., & Bredt, D. S. (1999). Synaptic targeting of the postsynaptic density protein PSD-95 mediated by lipid and protein motifs. *Neuron*, *22*(3), 497-509.

Zhang, Y., Matt, L., Patriarchi, T., Malik, Z. A., Chowdhury, D., Park, D. K., ... & Hell, J. W. (2014). Capping of the N-terminus of PSD-95 by calmodulin triggers its postsynaptic release. *The EMBO journal*, *33*(12), 1341-1353.

El-Husseini, A. E., Craven, S. E., Chetkovich, D. M., Firestein, B. L., Schnell, E., Aoki, C., & Bredt, D. S. (2000). Dual palmitoylation of PSD-95 mediates its vesiculotubular sorting, postsynaptic targeting, and ion channel clustering. *The Journal of cell biology*, *148*(1), 159-172.

Weber, P. C., Ohlendorf, D. H., Wendoloski, J. J., & Salemme, F. R. (1989). Structural origins of high-affinity biotin binding to streptavidin. *Science*, *243*(4887), 85-88.

Barker, D. F., & Campbell, A. M. (1981). The birA gene of Escherichia coli encodes a biotin holoenzyme synthetase. *Journal of molecular biology*, *146*(4), 451-467.

Beckett, D., Kovaleva, E., & Schatz, P. J. (1999). A minimal peptide substrate in biotin holoenzyme synthetase-catalyzed biotinylation. *Protein Science*, *8*(4), 921-929.

Schatz, P. J. (1993). Use of peptide libraries to map the substrate specificity of a peptide-modifying enzyme: a 13 residue consensus peptide specifies biotinylation in Escherichia coli. *Bio/technology*, *11*(10), 1138-1143.

Li, Y., & Sousa, R. (2012). Expression and purification of E. coli BirA biotin ligase for in vitro biotinylation. *Protein expression and purification*, *82*(1), 162-167.

CHAPTER 3: DESIGN AND PURIFICATION OF SOLUBLE PYK2 CONSTRUCTS ENCOMPASSING THE C-TERMINAL FUNCTIONAL DOMAINS

Shivani Sharma and Eric Underbakke

From the Roy J. Carver Department of Biochemistry, Biophysics and Molecular Biology, Iowa State University, Ames, Iowa 50011

Modified from a manuscript in preparation for bioRxiv

In collaboration with Tania Palhano Zanela

Abstract

The role of FAT (focal adhesion targeting) domain in the activation of Pyk2 is largely unknown. The regulatory core of Pyk2 contains an autoinhibitory FERM domain and central kinase. The C-terminal sequence of Pyk2 consists of a putatively disordered linker region capped by a small C-terminal FAT domain. There is considerable interest in investigating the regulatory mechanisms of the C-terminal Pyk2 regions. Previous studies implicate proline-rich repeat motifs in the C-terminal linker in scaffolding interactions (Bartos et al., 2010). In addition, the FAK FAT domain appears to stabilize FERM-mediated dimers (Cherrier et al., 2014). To date, our studies of the role of the Pyk2 C-terminal linker and FAT have been limited by difficulties of expressing and purifying the very large, partially disordered enzyme. Here, we report the design, engineering, and successful purification of recombinantly-expressed Pyk2 constructs encompassing the FERM, kinase, linker PRR, and FAT domains. These constructs were designed to promote solubility by limiting the intrinsically disordered sequences, while preserving as many PRR motifs as possible. We anticipate that these proteins will serve as a platform for future studies of Pyk2 PSD-95-mediated scaffolding and higher-order architecture due to FERM/FAT-mediated

dimerization.

Introduction

Structure-function studies into the mechanisms of regulation and activation of both FAK and Pyk2 have profited from the availability of readily purified recombinant constructs encompassing the regulatory, N-terminal FERM domain, a sixty-residue linker with the initial site of autophosphorylation (Y402 in Pyk2), and the catalytic kinase domain (**Figure 7A**). These FERM-kinase constructs have revealed critical regulatory interdomain interactions in FAK (via X-ray crystallography) and Pyk2 (via H/D exchange mass spectrometry) (Lietha et al., 2007, Loving & Underbakke, 2019).

Nevertheless, the C-terminal half of Pyk2 may also play important roles in the activation process. In both FAK and Pyk2, the approximately 185-residue linker C-terminal to the kinase exhibits multiple PRR motifs. The C-terminal linker is thought to be intrinsically disordered. The C-terminus of both FAK and Pyk2 is capped off by a FAT domain, a small antiparallel four-helix bundle. The FAK FAT domain is known to participate in FAK localization to plasma membrane focal adhesions through its interactions with paxillin and talin (Walkiewicz et al., 2015, Chen et al., 1995). The Pyk2 FAT domain may also promote focal adhesion targeting, but this role may be vestigial in cell types where Pyk2 localization is diffusively cytosolic (Schaller & Sasaki, 1997). Arnold and co-workers proposed additional roles for the FAK FAT domain in the higher-order multimerization of FAK at the focal adhesion. FAK structural models derived by X-ray crystallography and SAXS (small angle X-ray scattering) revealed a modest affinity dimerization interface between FERM F3 subdomains (Cherrier et al., 2014). The stability of the FERM-

mediated FAK dimerization is enhanced by the FAT domain, and SAXS models suggest that the C-terminal linker may wrap around monomers such that the FAT domain undergoes intermolecular interactions with the basic patch of the FERM F2 subdomain (**Figure 7B**) (Cherrier et al., 2014). FAK dimerization is likely involved in the activation mechanism, as point mutants abolishing the dimerization interface diminish autophosphorylation (Cherrier et al., 2014).

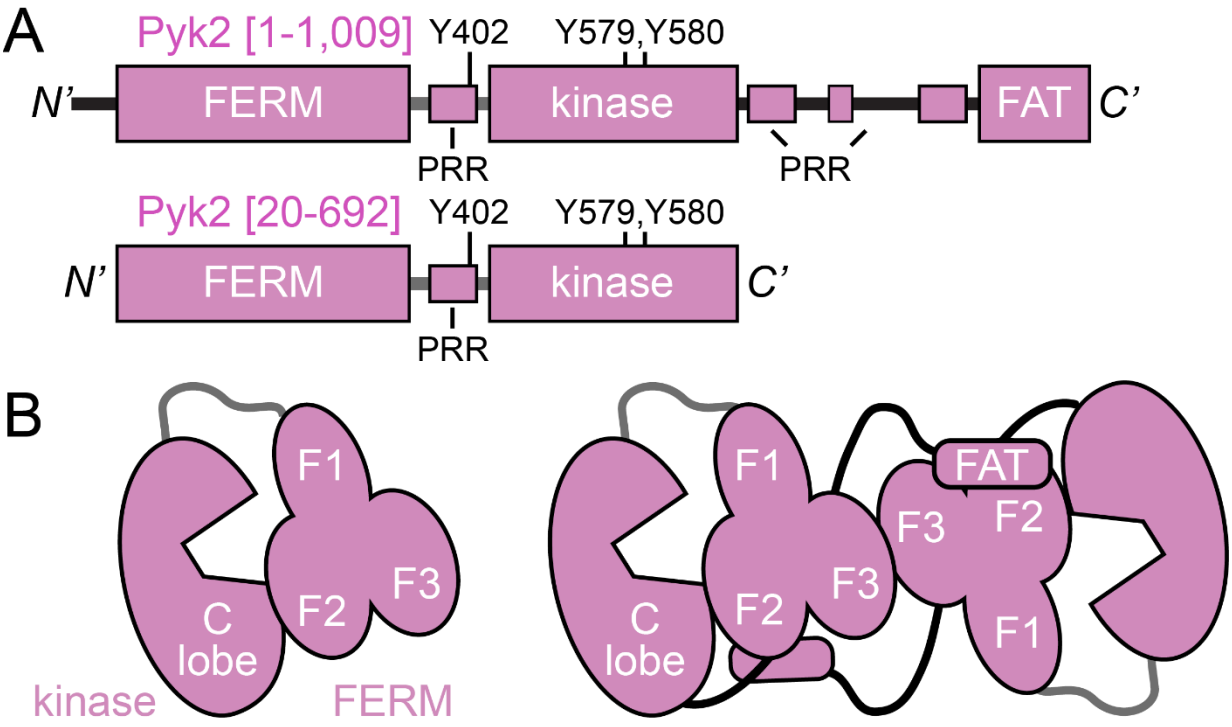

Figure 7. Possible regulatory roles of the Pyk2 FAT domain. **A**. Previously reported Pyk2 constructs (FERM—kinase, residues 20-692) that preserve the critical FERM-mediated regulation of the kinase omit PRR motifs in the putatively disordered C-terminal linker. **B**. Cartoon illustration highlighting how FERM—kinase constructs exhibit kinase C-lobe interactions with FERM F2 subdomain (left). Full-length Pyk2 may mimic higher-order interactions observed in FAK, wherein FERM dimerization (via F3 interactions) is stabilized by intermolecular FAT interactions with the FERM F2 basic patch (right).

The PRR motifs of the C-terminal linker also play important regulatory roles in FAK and Pyk2, serving to scaffold and coordinate other signaling proteins that include PRR-binding SH3 (Src homology 3) domains (Naser et al., 2018). FAK and Pyk2 scaffolding partners include the adaptor protein BCAR1 (Breast cancer anti-estrogen resistance protein 1/p130Cas), the GTPase-activating protein RhoGAP26 (or Graf, GTPase regulator with FAK), and some PI3K (phosphoinositide 3-kinase) family members (Avraham et al., 1995, Polte & Hanks, 1995, Dikic et al., 1996, Sasaki et al., 1995, Zhang et al., 2017) (see also Chapter 2). Importantly, the clustering elements of Pyk2 activation involve scaffolding interactions between one or more C-terminal PRR and the SH3 domain of PSD-95 (see also Chapter 2) (Seabold et al., 2003, Bartos et al., 2010).

Notably, both FAK and Pyk2 genes exhibit alternate transcriptional initiation sites to generate FRNK and PRNK (FAK- or Pyk2-related non-kinase), a truncated form missing the N-terminal FERM and kinase domains entirely (Schaller et al., 1993, Xiong et al., 1998). While the biological function of FRNK and PRNK is an emerging story, their competition with FAK and Pyk2 binding partners highlight the importance of the C-terminal linker and FAT domain.

Investigating the mechanistic roles of the Pyk2 C-terminal linker and FAT domain have been limited by difficulties in recombinant *Escherichia coli* expression and purification of full-length Pyk2. Functional full-length Pyk2 has been expressed and isolated from *E. coli* via immunoprecipitation (Bartos et al., 2010), but structure-function investigations require larger quantities. Large, multidomain proteins are a challenge for *E. coli* expression. Loosely structured linkers tend to aggregate during expression. In addition, post-lysis proteolysis by endogenous periplasmic *E. coli* proteases of interdomain linkers complicates isolation of intact protein. Here,

we attempt to circumvent expression and purification challenges for Pyk2 with several modifications to the constructs. First, gene codons were optimized to favor *E. coli* tRNA usage. Second, aggregation prone N-terminal (pre-FERM) residues were truncated. Third, segments of the long C-terminal linker were shortened while preserving most PRR motifs. We report the successful engineering and purification of two such constructs herein. Yields are sufficient to enable future studies focused on Pyk2 PSD-95-mediated scaffolding and the activity and higher-order architecture due to FERM/FAT-mediated dimerization.

Materials and Methods

Materials

The cloning vector pET-H6-SUMO-TEV-LIC (1S) received from Scott Gradia (Addgene, 29659) as a gift. The His_6-SUMO-tagged, codon-optimized Pyk2 [20-1009] expression vector pNAM007 was cloned by Natalie McClure (Underbakke lab).

Generating optimized Pyk2 FERM-kinase-linker-FAT expression constructs

The 'Round the Horn PCR-based mutagenesis strategy was used to truncate the C-terminal linker in the expression vector pNAM007 encoding Pyk2 residues 20-1009. Primers used to generate pSS007 (Pyk2 residues 20-729, 868-1009) and pSS008 (Pyk2 residues 20-768, 868-1009) are listed in **Table 2**. The forward primer SS143 joining the FAT domain (residues 868-1009) was used in the 'Round the Horn PCR for both constructs.

Table 2. Primers for PCR-based in-frame deletion of C-terminal linker segments Δ730-867 or Δ769-867 to generate pSS007 and pSS008, respectively.

Primer Name	Description	Sequence (3' to 5')
SS143	Forward pSS007 primer	CTGTTCCAGCAGGCACGCTAGGTTCAACCGGCACCCAAC
SS144	Reverse pSS007 primer	GGCGGGGTTTATAGCGGGCGGTGGGGTTTGGTTG
SS145	Reverse pSS008 primer	GGTAGAGGCCAGTTGAGGGAAGTGTGTGGTGGGAATG

The primers were prepared for downstream ligation by 5' phosphorylation using T4 polynucleotide kinase (PNK) incubated with 10 mM ATP at 37 °C for 30 min. PNK was heat inactivated at 65 °C for 20 min. Primer pairs were used to amplify template pNAM007 using standard PCR conditions for Phusion DNA polymerase (New England Biolabs). Expected product sizes (Y.YY kbp and Z.ZZ kbp for pSS007 and pSS08, respectively) were checked by diagnostic 0.8% DNA agarose gel. Successful PCR reactions were pooled, and template was digested using DpnI restriction enzyme. Linear PCR product was purified by resolving on a agarose gel and extraction using the Wizard SV Gel Clear-Up System (Promega). Gel-extracted PCR product was circularized using T4 DNA ligase (Thermo Scientific) with an 18 hrs, 25 °C incubation. The ligation reaction was transformed into DH5α chemically competent *E. coli* by heat shock transformation. Transformants were selected by plating on LB supplemented with 50 µg/mL kanamycin. Kanamycin-resistant transformants were grown in small kanamycin-supplemented LB cultures, and plasmids were isolated using Wizard Plus SV Miniprep kits (Promega). Successful truncation was confirmed using DNA sequencing. Successful Pyk2 open reading frames encoding residues 20-729/868-1009 and 20-768/868-1009 were designated pSS007 and pSS008, respectively (**Figure 8**).

Protein purification of pSS007 and pSS008

Expression plasmids pSS007 and pSS008 encoding pET-H6-SUMO-Pyk2 [20-729/868-1009] and pET-H6-SUMO-Pyk2 [20-768/868-1009], respectively, were transformed into BL21(DE3) cells. Starter cultures were grown overnight at 37 °C using LB medium containing 50 µg/mL kanamycin. The starter culture was used to inoculate four 1 L expression cultures (1:100) of LB with 50 µg/mL kanamycin. Expression cultures were grown at 37°C with continuous shaking until they reach an OD_{600nm} of 0.30, when the temperature was decreased to 18 °C. Once cells reached an OD_{600nm} of 0.5, the cells were induced with 1 mM isopropyl β-D-1-thiogalactopyranoside and left to shake overnight at 18 °C. Harvesting of cells was performed after an 18 hr induction using centrifugation at 4,200 ×g for 20 min. Cell pellets were stored at −80°C until used for purification.

Harvested cells were thawed after addition of lysis buffer (150 mM NaCl, 50 mM HEPES, 15 mM imidazole, 1 mM phenylmethylsulfonyl fluoride, 20 mM EDTA, 5% glycerol, and 5 mM 2-mercaptoethanol (2-ME) pH 8). Cells were lysed using sonication, and lysate was centrifuged at 20,000 ×g for 45 min at 4 °C to remove cell debris. Cleared lysate was applied to a 2 mL HisPur Ni-NTA Superflow agarose column (Thermo Scientific) pre-equilibrated in binding buffer [150 mM NaCl, 50 mM HEPES, 20 mM imidazole, 5% glycerol, and 5 mM 2-ME pH 8]. The Ni-NTA column was washed with 12 column volumes of wash buffer (250mM NaCl, 50mM HEPES, 5% glycerol, 20mM imidazole, and 5 mM 2-ME pH 8). His_6-SUMO-tagged Pyk2 was eluted with high-imidazole elution buffer (150 mM NaCl, 50 mM HEPES, 150 mM imidazole, 5% glycerol, and 5 mM 2-ME pH 8). Protein-containing fractions were dialyzed for 3 hr with His_6-Ulp1, a SUMO-specific protease, against dialysis buffer (50 mM Tris pH 7.8, 100 mM KCl, 5% glycerol, 1

mM DTT). A subtractive run through the Ni-NTA column pre-equilibrated in binding buffer followed for the removal of purification tags and proteases. Pyk2 constructs were buffer-exchanged via passage through a Bio-Scale Mini Bio-Gel P-6 desalting cartridge (Bio-Rad) pre-equilibrated in storage buffer (150 mM NaCl, 50 mM HEPES, 10% glycerol, and 1 mM DTT pH 7.4). Protein was concentrated using a Spin-X concentrator of 10k MWCO (Corning), aliquoted, and snap-frozen in liquid N_2. Protein stocks were stored at −80 °C.

Results and discussion

Previous attempts to purify recombinantly-expressed full-length Pyk2 were hampered by cytotoxicity and protein aggregation during expression (Sharma, data not shown). While N-terminal SUMO tag fusion markedly improved yields of a FERM—kinase construct (**Figure 7A**), the solubility tag was insufficient to improve full-length Pyk2 yields. Codon optimization did not improve yields. Low temperature (12-18 °C) expression also failed to produce soluble full-length Pyk2. Co-expression with psychrophilic chaperones (e.g., ArcticExpress(DE3) *E. coli*, Agilent) was also unsuccessful. Insect cell expression using baculovirus transduction did yield soluble Pyk2, but yields were not sufficient for downstream structural studies (Loving & Underbakke, unpublished results).

To generate a useful Pyk2 recombinant expression construct encoding as much of the native sequence as possible, we turned to minimalistic gene truncation. The first nineteen residues of FAK are apparently unstructured and aggregation-prone (Ceccarelli et al., 2006), therefore we began by truncating the full-length Pyk2 (residues 1—1009) by nineteen residues

(Δ19, residues 20-1009) to generate the codon-optimized construct pNAM007 (**Figure 8**, Natalie McClure, unpublished results). However, all the aforementioned expression conditions failed to yield soluble, functional Pyk2 (Sharma, data not shown).

We suspected that the putatively unstructured C-terminal linker was seeding aggregation during *E. coli* expression. Indeed, constructs omitting the C-terminal sequence are well-folded and functional (**Figure 7A**). However, our ultimate goal to study the scaffolding and regulatory roles of C-terminal features such as the PRRs and FAT domain precluded total removal. Hence, we turned to sequence truncation in linker sequences with few known functions (**Figure 8**). We employed PCR-based gene editing ('Round the Horn strategy) to generate two constructs (pSS007, Δ730-867 and pSS008, Δ769-867) that preserved most PRR motifs and the C-terminal FAT domain. The final expression constructs encoded codon optimized His_6-SUMO-Pyk2 residues 20-729/868-1009 and 20-768/868-1009, for pSS007 and pSS008, respectively.

Expression conditions (temperature and time) were optimized until soluble, functional pseudo-full-length Pyk2 was obtained from both constructs. Briefly, immobilized metal-affinity chromatography (IMAC) enriched for the soluble His_6-tagged Pyk2 constructs (**Figure 9**). Incubation with the SUMO-specific protease Ulp1 removed the non-native His_6-SUMO tag, followed by protease and tag removal with a subtractive IMAC run (**Figure 9**). Protein stocks were obtained with concentrations up to 35 µM. Final protein stocks are enriched, yet incompletely purified. Lower molecular weight bands likely correspond to N-terminal (i.e., His-tag containing) proteolytic fragments of the Pyk2 constructs. Protease-deficient cell lines (BL21-

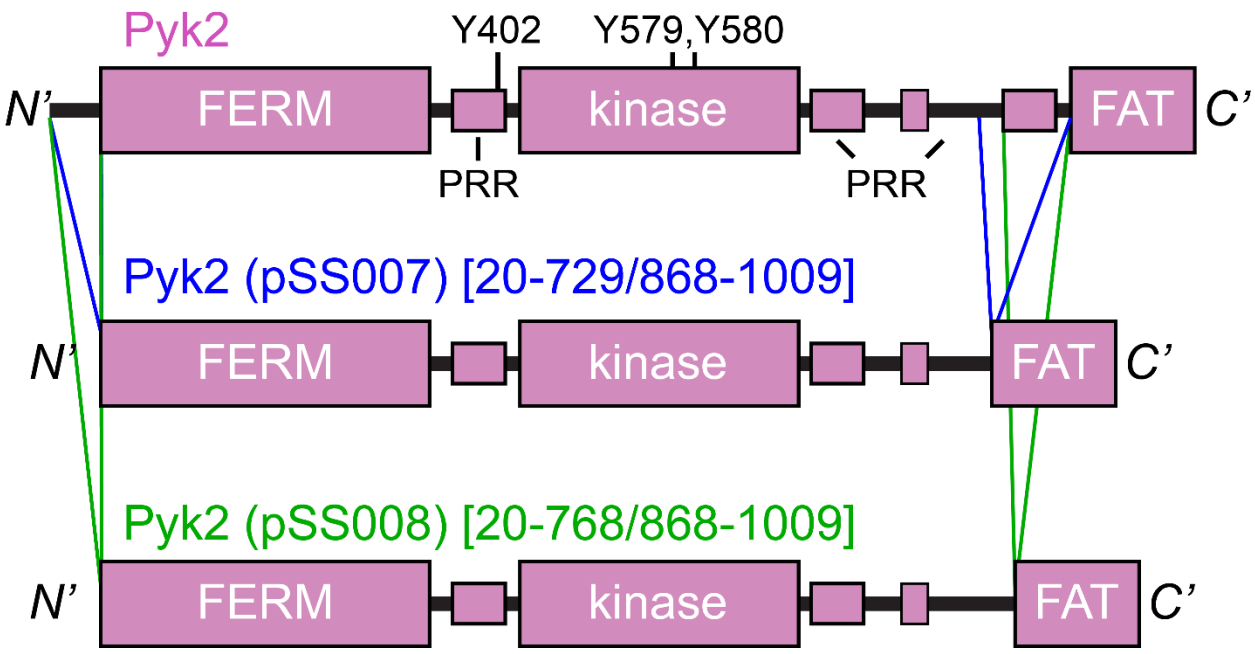

Figure 8. Design of Pyk2 C-terminal linker truncations encompassing PRR and FAT domains. Expression vectors with N-terminal truncation (Δ1-19) and various C-terminal linker truncations (Δ730-867 or Δ769-867) were engineered to promote solubility upon recombinant expression in *E. coli* while preserving putatively important regulatory features, such as C-terminal PRR motifs and the FAT domain.

derivatives, *lon*/*ompT*) and protease inhibitors (i.e., serine protease inhibitor phenylmethylsulfonyl fluoride and, for early prep stages, metalloprotease inhibitor EDTA) were employed for the purification process, but the multiple solvent exposed linker sequences are highly vulnerable to endogenous *E. coli* periplasmic and outer membrane proteases. Future purifications will focus on combating endogenous proteases using a more comprehensive battery of *E. coli*-customized protease inhibitors.

Importantly, Western blotting with anti-phosphotyrosine-specific antibody revealed extensive autophosphorylation of both constructs (data not shown). The autophosphorylation during protein expression reveals that the Pyk2 constructs retain kinase activity, as *E. coli* do not harbor endogenous tyrosine kinases.

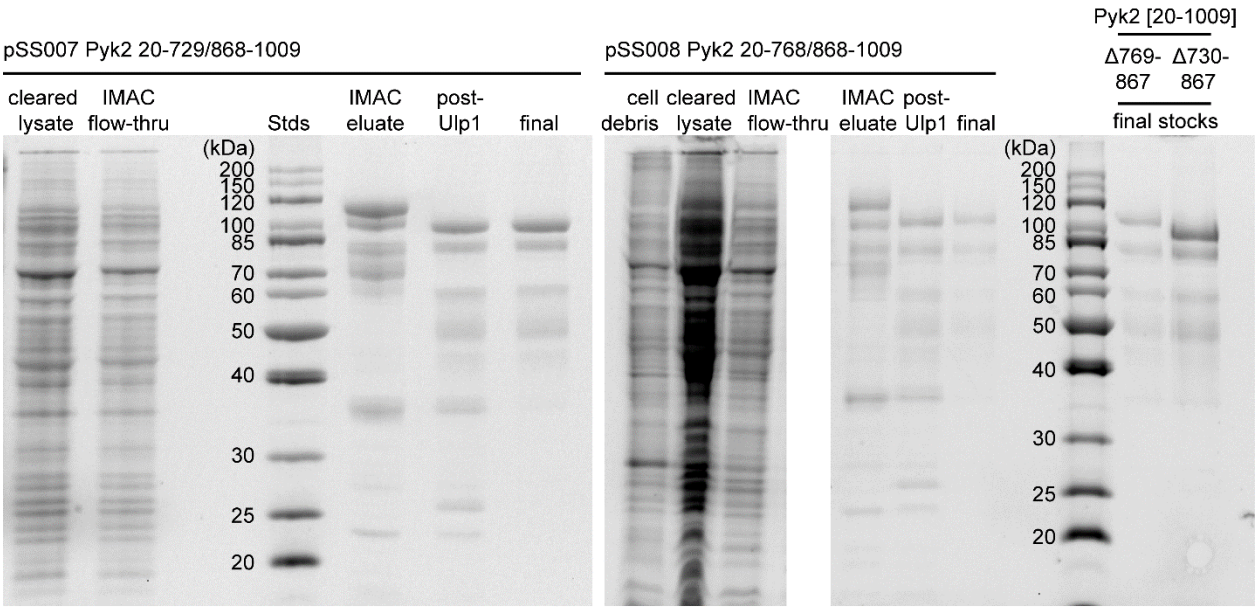

Figure 9. SDS-PAGE analysis of pseudo-full-length Pyk2 enriched from expression constructs pSS007 and pSS008. Purification fractions and final proteins stocks were resolved in 12% SDS-PAGE and stained using tryptophan-specific fluorophore 2,2,2-trichloroethanol. Expected molecular weights (MW) of Pyk2 [20-729/868-1009] (pSS007) were 110.721 kDa and 97,772 kDa, pre- and post-His_6-SUMO tag removal, respectively. Expected MW of Pyk2 [20-768/868-1009] (pSS008) were 114.865 kDa and 101.916 kDa, pre- and post-tag removal.

Ultimately, we succeeded in engineering, optimizing, and enriching for nearly full-length Pyk2 encompassing the major regulatory and localizations domains—FERM, kinase, and FAT—plus the majority of the PRR motifs in the linker regions. These pseudo-full-length Pyk2 constructs are the first to be purified to concentrations suitable for structure-function studies. We anticipate that these constructs will serve as a foundation for future experiments exploring the role of PRR motifs in PSD-95 scaffolding (see also Chapter 2) and proposed regulatory roles for the FAT domain in the higher-order activation complex

References

Schaller, M. D., & Parsons, J. T. (1994). Focal adhesion kinase and associated proteins. Current opinion in cell biology, 6(5), 705-710

McGee, A. W., & Bredt, D. S. (1999). Identification of an intramolecular interaction between the SH3 and guanylate kinase domains of PSD-95. Journal of Biological Chemistry, 274(25), 17431-17436.

McGee, A. W., Dakoji, S. R., Olsen, O., Bredt, D. S., Lim, W. A., & Prehoda, K. E. (2001). Structure of the SH3-guanylate kinase module from PSD-95 suggests a mechanism for regulated assembly of MAGUK scaffolding proteins. Molecular cell, 8(6), 1291-1301.

Shin, H., Hsueh, Y. P., Yang, F. C., Kim, E., & Sheng, M. (2000). An intramolecular interaction between Src homology 3 domain and guanylate kinase-like domain required for channel clustering by postsynaptic density-95/SAP90. Journal of Neuroscience, 20(10), 3580-3587.

Brami-Cherrier, K., Gervasi, N., Arsenieva, D., Walkiewicz, K., Boutterin, M., Ortega, A., . . . Arold, S. (2014, 2 18). FAK dimerization controls its kinase-dependent functions at focal adhesions. EMBO Journal, 33(4), 356-370.

Bartos, J., Ulrich, J., Li, H., Beazely, M., Chen, Y., MacDonald, J., & Hell, J. (2010, 1 13). Postsynaptic clustering and activation of Pyk2 by PSD-95. *Journal of Neuroscience, 30*(2), 449-463.

Naser, R., Aldehaiman, A., Díaz-Galicia, E., & Arold, S. T. (2018). Endogenous control mechanisms of FAK and PYK2 and their relevance to cancer development. *Cancers*, *10*(6), 196.

Chen, H. C., Appeddu, P. A., Parsons, J. T., Hildebrand, J. D., Schaller, M. D., & Guan, J. L. (1995). Interaction of focal adhesion kinase with cytoskeletal protein talin. *Journal of Biological Chemistry*, *270*(28), 16995-16999.

Schaller, M. D., & Sasaki, T. (1997). Differential signaling by the focal adhesion kinase and cell adhesion kinase β. *Journal of Biological Chemistry*, *272*(40), 25319-25325.

Walkiewicz, K. W., Girault, J. A., & Arold, S. T. (2015). How to awaken your nanomachines: Site-specific activation of focal adhesion kinases through ligand interactions. *Progress in biophysics and molecular biology*, *119*(1), 60-71.

Ceccarelli, D. F., Song, H. K., Poy, F., Schaller, M. D., & Eck, M. J. (2006). Crystal structure of the FERM domain of focal adhesion kinase. *Journal of Biological Chemistry*, *281*(1), 252-259.

Loving, H. S., & Underbakke, E. S. (2019). Conformational dynamics of FERM-mediated autoinhibition in Pyk2 tyrosine kinase. *Biochemistry*, *58*(36), 3767-3776.

Lietha, D., Cai, X., Ceccarelli, D. F., Li, Y., Schaller, M. D., & Eck, M. J. (2007). Structural basis for the autoinhibition of focal adhesion kinase. *Cell*, *129*(6), 1177-1187.

Schaller, M. D., Borgman, C. A., & Parsons, J. T. (1993). Autonomous expression of a noncatalytic domain of the focal adhesion-associated protein tyrosine kinase pp125FAK. *Molecular and cellular biology*, *13*(2), 785-791.

Seabold, G. K., Burette, A., Lim, I. A., Weinberg, R. J., & Hell, J. W. (2003). Interaction of the tyrosine kinase Pyk2 with the N-methyl-D-aspartate receptor complex via the Src homology 3 domains of PSD-95 and SAP102. *Journal of Biological Chemistry*, *278*(17), 15040-15048.

Polte, T. R., & Hanks, S. K. (1995). Interaction between focal adhesion kinase and Crk-associated tyrosine kinase substrate p130Cas. *Proceedings of the National Academy of Sciences*, *92*(23), 10678-10682.

Avraham, S., London, R., Fu, Y., Ota, S., Hiregowdara, D., Li, J., ... & Avraham, H. (1995). Identification and characterization of a novel related adhesion focal tyrosine kinase (RAFTK) from megakaryocytes and brain. *Journal of Biological Chemistry*, *270*(46), 27742-27751.

Dikic, I., Tokiwa, G., Lev, S., Courtneidge, S. A., & Schlessinger, J. (1996). A role for Pyk2 and Src in linking G-protein-coupled receptors with MAP kinase activation. *Nature*, *383*(6600), 547-550.

Sasaki, H., Nagura, K., Ishino, M., Tobioka, H., Kotani, K., & Sasaki, T. (1995). Cloning and characterization of cell adhesion kinase β, a novel protein-tyrosine kinase of the focal adhesion kinase subfamily. *Journal of Biological Chemistry*, *270*(36), 21206-21219.

Zhang, J., Gao, X., Schmit, F., Adelmant, G., Eck, M. J., Marto, J. A., ... & Roberts, T. M. (2017). CRKL mediates p110β-dependent PI3K signaling in PTEN-deficient cancer cells. *Cell reports*, *20*(3), 549-557.

Xiong, W. C., Macklem, M., & Parsons, J. T. (1998). Expression and characterization of splice variants of PYK2, a focal adhesion kinase-related protein. *Journal of cell science*, *111*(14), 1981-1991.

CHAPTER 4: CONCLUSIONS AND FUTURE DIRECTIONS

We successfully designed, expressed, and purified a full length Pyk2 construct with two versions of Kinase-FAT linker, retaining the polyproline regions in both. We designed N and C terminus Avi tagged PSD-95 constructs and expressed and purified them in *E.coli*. The Avi tagged PSD-95 system can be used for future pull down and SPR experiments in conjunction with the full length Pyk2.

Pyk2 although very similar to FAK structurally and sequence wise, not much is known about it and its activation mechanism. The presence of Pyk2 in the post synaptic density makes it a remarkable candidate to be studied as a prerequisite to understanding and regulating signaling pathways. The overall understanding of roles played by FAT domain in the context of activation are far less understood. The interesting anti-parallel four helix bundle structure formed by FAT domains due to domain swapping (Fang et al., 2014) might confer it additional functions. Additionally, interaction of FAT domain with the FERM domain as a mechanism to stabilize the autoinhibitory structure (Fang et al., 2014) points towards an indirect role in activation.

References

Fang, X., Liu, X., Yao, L., Chen, C., Lin, J., Ni, P., ... & Fan, Q. (2014). New insights into FAK phosphorylation based on a FAT domain-defective mutation. *PloS one*, *9*(9).